IPSCS-DERIVED NESCS FOR NEUROREGENERATION IN MJD

Daniel Alexandre Sousa Henriques

Tese no âmbito do Mestrado de Biologia Celular e Molecular orientada pela Doutora Liliana Simões Mendonça (Centro de Neurociências e Biologia Celular, Universidade de Coimbra) e sob orientação interna do Professor Doutor Carlos Jorge Alves Miranda Bandeira Duarte (Departamento de Ciências da Vida, Universidade de Coimbra) e apresentada ao Departamento de Ciências da Vida da Universidade de Coimbra.

Agosto de 2018

UNIVERSIDADE D
COIMBRA

The present work was performed in the Vectors and Gene Therapy group of the Center for Neuroscience and Cell Biology (University of Coimbra), headed by Professor Luís Pereira de Almeida, and under the supervision of Doctor Liliana Simões Mendonça (Center for Neuroscience and Cell Biology, University of Coimbra) and internal supervisor Doctor Carlos Jorge Alves Miranda Bandeira Duarte (Department of Life Sciences, University of Coimbra)

This work was supported by the European Union through the European social fund, funds FEDER through COMPETE, POPH and QREN; the National Ataxia Foundation; the French Muscular Dystrophy Association (AFM-Téléthon, Trampoline Grant#20126), by SynSpread; 2013 JPND Transnational call Ref. JPND-CD/0001/2013 and the Portuguese Government by national funds through the Portuguese Foundation for Science and Technology (FCT), project POCI-01-0145-FEDER-030737.

Acknowledgments/Agradecimentos

Primeiramente, gostaria de agradecer ao Professor Doutor Luís Almeida por me ter recebido no seu laboratório para a realização deste trabalho. Agradecer todo o tempo despendido, sempre com um sorriso e simpatia, disposto a ajudar em qualquer problema, liderando e mantendo organizado um grupo tão grande como o seu.

Gostaria, claro, de agradecer profundamente à Doutora Liliana Mendonça por ter acreditado nas minhas capacidades, por me ter aceite para fazer parte do seu projeto, por me ensinar tudo o que sei a nível de trabalho laboratorial e me ter ajudado durante todo este ano. Sempre presente e disposta a ajudar em tudo o que fosse necessário relacionado ou não com o trabalho, apesar da sua agenda bastante ocupada. Mais do que orientadora, foi uma amiga que acompanhou todo o meu trabalho durante todo o ano, mantendo um ambiente saudável e divertido com os seu alunos, ajudando certamente a ultrapassar quaisquer dificuldades que pudessem surgir.

Quero agradecer também ao Ricardo Moreira não só por toda a sua ajuda e espírito de entreajuda durante este ano, que definitivamente facilitou este ano difícil, mas principalmente pela sua amizade. Uma amizade que, desde o primeiro dia, ultrapassou as barreiras do laboratório e que certamente será uma amizade duradoura.

Não posso deixar também de agradecer às restantes pessoas da “sala de mestrados”, principalmente à Beatriz, à Carina, à Inês, à Jéssica, ao José Pedro, à Mariana, ao Patrick, ao Ricardo, à Rita e à Tânia, pela companhia e amizade ao longo deste ano. Agradecimento especial à minha colega de mesa Carina Henriques que, por vezes, prontamente me disponibilizou um terço da sua mesa.

Quero deixar uma palavra de agradecimentos também à Sandra pela ajuda no meu período inicial de adaptação e aprendizagem à vida de laboratório e pela amizade que daí surgiu.

Agradeço também a todos os membros do Grupo LA, que sempre se mostraram disponíveis para ajudar e me receberam no seu meio de braços abertos.

Houve também um conjunto de pessoas que me acompanharam este ano, fora do laboratório. Palavra especial para todos os membros dos Baldes, que não só este ano mas em todos os 6 anos da minha vida universitária estiveram sempre lá e que são as melhores pessoas que orgulhosamente posso chamar de amigos para a vida. Deixo também um agradecimento aos restantes amigos de Biologia e BCM, principalmente à minha “família”;

Ana Carolina, André Barbosa, Carolina Figueiredo, Jorge Silva e Mariana Pais por também me terem acompanhado nesta fase da minha vida e certamente que continuarão a acompanhar-me por muitos anos. Agradeço também a todos os meus amigos que de certa forma ainda nao foram mencionados mas que sao igualmente importantes, especialmente ao Afonso Eliseu, à Ângela Rebelo, à Carolina Rocha, à Diana Callebaut e ao José Silvestre pela sua amizade e companhia.

Por fim quero agradecer a toda a minha familia e dedicar esta tese aos meus pais, por todo o apoio que sempre me deram e me terem permitido aqui chegar. Sem eles nada disto seria possível e certamente têm o papel mais importante na minha jornada.

Muito obrigado a todos.

Index

Abbreviations

AD - Alzheimer's disease

BDNF - Brain-derived neurotrophic factor

BMP - Bone morphogenetic protein

BSA - Bovine Serum Albumin

DMEM - Dulbecco's Modified Eagle's medium

DMEM/F12 - Dulbecco's Modified Eagle Medium: Nutrient Mixture F-12

DRPLA - Dentatorubral Pallidoluysian Atrophy

DTT - Dithiothreitol

EDTA - Ethylenediaminetetraacetic acid

ESCs - Embryonic stem cells

FSK - Forskolin

GDNF - Glial cell-derived neurotrophic factor

GFAP - Glial Fibrillary Acidic protein

GFP - Green fluorescent protein

HD - Huntington’s disease

Iba1 - Ionized calcium-Binding Adapter molecule 1

iNs - Induced neurons

iPSCs - Induced pluripotent stem cells

KDa - Kilo Dalton

MAP2 - Microtubule associated protein 2

MJD - Machado-Joseph disease

NESCs - Neuroepithelial stem cells

NG2 - Neural/glial antigen 2

NGF - Nerve growth factor

NGS - Normal goat serum

PBS - Phosphate-buffered saline

PD - Parkinson's disease

PFA - Paraformaldehyde

PMA - Purmorphamine

PMSF - Phenylmethane sulfonyl fluoride

PolyQ - Polyglutamine

PSCs - Pluripotent Stem Cell

PSD-95 - Postsynaptic density protein 95

PVDF - Polyvinylidene fluoride

Ripa – Radio-Immunoprecipitation Assay

RISC - RNA-induced silencing complex

SBMA - Spinal and Bulbar Muscular Atrophy

SCA - Spinocerebellar ataxia

SCA3 - Spinocerebellar ataxia type 3

SDS - Sodium dodecyl sulfate

SHH - Sonic hedgehog

TBS - Tris-buffered saline

TGFB - Transforming growth factor beta

UPS - Ubiquitin-Proteasome System

VGLUT1 - Vesicular glutamate transporter 1

VPA - Valproic acid

List of tables and figures

List of Tables

List of Figures

Abstract

Spinocerebellar Ataxia Type 3 (SCA3), also known as Machado-Joseph disease (MJD), is an autosomal dominant neurodegenerative disease. MJD arises from a mutation in the *MJD1/ ATXN3* gene, in which an increased number of the trinucleotide CAG results in an expanded polyglutamine tract in the Ataxin-3 protein. The mutated *ATXN3* gene has 55-87 CAG repeats, while the normal gene has 10-51 repeats. MJD is characterized by extensive neuronal death, affecting mainly the cerebellar system, as well as the pyramidal, extrapyramidal, motor neuron and oculomotor systems. The most common symptoms presented by patients are impaired motor coordination, dysarthria and dysphagia, and presently there is no therapy available to stop or delay the progression of this disease.

Cell therapies hold the promise to replace impaired and death neurons. Induced pluripotent stem cells (iPSCs) are obtained by reprogramming somatic cells into pluripotent cells. The iPSCs are then induced into cells of the neuroectoderm, namely neuroepithelial stem cells (NESCs) that upon differentiation give rise to cells of the nervous system. NESCs have been successfully used for cell replacement strategies in mouse models of neurodegenerative diseases as Parkinson´s disease.

In the present study we aimed to assess the potential of human iPSCs-derived NESCs to be used as a cell-replacement and neuroprotective strategy in neurodegenerative diseases as MJD. Thus, four cell lines established in the lab (one cell line of NESCs obtained from a control and three cell lines of NESCs obtained from MJD patients) were thoroughly characterized. The multipotency of the obtained cells was assessed, namely the ability to give rise to glia cells and functional neurons upon differentiation. It was evaluated whether the cell lines of MJD patients have differences on the neuronal functionality, namely neurites length and number of functional synapses. Our results indicate that upon differentiation human iPSCs-derived NESCs give rise to glial cells and functional neurons, and no impairments in neuronal functionality were observed for the cell lines of MJD patients. Additionally, NESCs were transplanted into the cerebellum of adult NOD.scid mice. It was observed that two months upon transplantation the NESCs survived and were able to differentiate into neurons and glial cells, without major signs of immune rejection. Thus, results reveal that iPSCs-derived NESCs have potential to be used in cell replacement and neuroprotective strategies in MJD.

Keywords: Spinocerebellar ataxia type 3 (SCA3), Mutant Ataxin-3, NESCs, iPSCs, Transplantation.

Resumo

A ataxia espinocerebelosa do tipo 3 (SCA3), também conhecida como doença de Machado-Joseph (MJD), é uma doença neurodegenerativa autossómica dominante. A MJD tem como causa uma mutação no gene *MJD1/ATXN3,* no qual uma expansão do trinucleótido CAG resulta na presença de um tracto de poliglutamina expandido na proteina ataxina-3. O gene *ATXN3* mutado apresenta 55-87 repetiçoes do trinucleótido CAG, enquanto que o gene normal apresenta apenas 10-51 repetiçoes. A MJD é caracterizada por uma extensa morte neuronal, afectando principalmente o cerebelo, assim como os sistemas piramidal, extrapiramidal, oculomotor e neurónios motores. Os sintomas mais commummente apresentados pelos pacientes incluem coordenação motora comprometida, disartria e disfagia, não existindo atualmente terapias capazes de parar ou atrasar a progressão da doença.

Estratégias de terapia celular apresentam grande potencial na substituição de neurónios comprometidos ou mortos. Células estaminais pluripotentes induzidas (iPSCs) são obtidas através da reprogramação de células somáticas em células pluripotentes. Estas iPSCs são subsequentemente induzidas em células da neuroectoderme, nomeadamente células estaminais neuroepiteliais (NESCs) que após diferenciação dão origem a células do sistema nervoso. NESCs já foram utilizadas em estratégias de terapia celular, visando a substituição celular, em modelos de murganho de doenças neurodegenerativas como a doença de Parkinson.

No presente trabalho temos como objetivo avaliar o potencial de células estaminais neuroepiteliais derivadas de células estaminais pluripotentes induzidas humanas, para serem usadas em estratégias de substituição celular e neuroprotectoras em doenças neurodegenerativas como a MJD. Deste modo, quatro linhas celulares foram estabelecidas (uma linha celular de NESCs controlo e três linhas de NESCs obtidas de pacientes com MJD) e foram minuciosamente caracterizadas. A sua multipotencia foi analisada, nomeadamente a capacidade de dar origem a neurónios funcionais assim como células da glia após diferenciação. Foi também avaliado se estas linhas celulares apresentavam diferenças a nível de funcionalidade neuronal, nomeadamente o tamanho das neurites bem como o número de sinapses. Os nossos resultados indicam que as células estaminais neuroepiteliais derivadas de células estaminais pluripotentes induzidas humanas são capazes de se diferenciarem em neurónios funcionais e células da glia não tendo sido observadas disfunções neuronais nas linhas celulares obtidas de pacientes com MJD. Adicionalmente, NESCs foram transplantadas no cerebelo de murganhos NOD.scid. Dois meses após o transplante, observamos que as NESCs transplantadas sobreviveram e

foram capazes de se diferenciarem em neurónios e células da glia, sem a presença de grandes sinais de rejeição do transplante. Assim, os resultados do presente trabalho revelam que células estaminais neuroepiteliais derivadas de células estaminais pluripotentes induzidas humanas têm grande potencial para serem usadas em estratégias de terapia celular no tratamento da doença de Machado-Joseph.

Palavras-chave: Ataxia espinocerebelosa do tipo 3 (SCA3), ataxina-3 mutante, NESCs, iPSCs, Transplantação.

Chapter I - Introduction

1. Polyglutamine diseases

Polyglutamine (PolyQ) diseases are a group of neurodegenerative disorders caused by an increased number of the cytosine-adenine-guanine (CAG) triplet in a disease-specific gene, which is translated into an abnormal tract of the amino acid glutamine in its protein, resulting in an pathogenic expanded polyglutamine tract (Bauer and Nukina, 2009). This group includes 6 Spinocerebellar Ataxias (SCA 1, 2, 3, 6, 7 and 17), Huntington's disease (HD), Dentatorubro pallidoluysian atrophy (DRPLA) and Spinal and bulbar muscular atrophy (SBMA). All of these diseases, but the last one, are autosomal dominantly inherited (Fan et al., 2014) and HD and SCA3 have the highest worldwide prevalence (Schols et al., 2004).

Each disease of the "PolyQ diseases" group has its own causative gene (Fan et al., 2014) and, the number of repeats at which the polyglutamine tract in the associated protein becomes pathological varies from one to another. For example, the *CACNA1A* gene is the gene involved in SCA6 pathology and, 21 to 27 CAG repeats are enough to trigger the disease (Zhuchenko et al., 1997). While in Huntington's disease, the Huntingtin gene only becomes pathological with 36 or more CAG repeats (Rubinsztein et al., 1996).

These diseases present heterogeneous symptoms that usually start in midlife and frequently progress to fatal neuronal loss in specific brain regions, which is caused by the neuronal accumulation of mutant proteins (Fan et al., 2014). The age of onset is reported to be dependent on the number of CAG repeats (Budworth and McMurray, 2013; Langbehn et al., 2010; Ranum et al., 1994).

Table 1. Nine PolyQ diseases and its biologic features (Matos et al., 2011).

Disease name	Mutated gene	Protein product	Putative function	CAG repeat size		Regions most affected
				Normal	Pathogenic	
HD	*HD*	Huntingtin	Signaling, transport, transcription	6–34	36–121	Striatum, cerebral cortex
DRLPA	*DRPLA*	Atrophin 1	Transcription	7–34	49–88	Cerebellum, cerebral cortex, basal ganglia, Luys body
SBMA	*AR*	Androgen receptor	Steroid-hormone receptor	9–36	38–62	Anterior horn and bulbar neurons, dorsal root ganglia
SCA1	*SCA1*	Ataxin-1	Transcription	6–39	40–82	Cerebellar Purkinje cells, dentate nucleus, brainstem
SCA2	*SCA2*	Ataxin-2	RNA metabolism	15–24	32–200	Cerebellar Purkinje cells, brainstem, frontotemporal lobes
SCA3	*ATXN3/ MJD/SCA3*	Ataxin-3	Deubiquitinating activity and transcription regulation	10–51	55–87	Cerebellar dentate neurons, basal ganglia, brainstem, spinal cord
SCA6	*CACNA1A*	$CACNA1_A$	P/Q-type α1A calcium channel subunit	4–20	20–29	Cerebellar Purkinje cells, dentate nucleus, inferior olive
SCA7	*SCA7*	Ataxin-7	Transcription	4–35	37–306	Cerebellum, brainstem, macula, visual cortex
SCA17	*SCA17*	TBP	Transcription	25–42	47–63	Cerebellar Purkinje cells, inferior olive

1.1. Spinocerebellar ataxias

Spinocerebellar ataxias (SCAs) are a group of dominantly inherited progressive neurodegenerative disorders characterized by motor impairments with cerebellar origin (cerebellar ataxia) (Jacobi et al., 2011). There are more than 25 subtypes of SCAs numbered chronologically in order of discovery of the triggering gene (Paulson, 2009). In this large group of SCAs only a few of them are also polyglutamine diseases. Thus, 6 SCAs (SCA 1, 2, 3, 6, 7 and 17) are caused by an increased number of CAG repeats; although the majority are caused by missense mutations leading to protein dysfunctions (Manto, 2005). For example, SCA 4 is caused by a mutation in chromosome 16, while SCA 8 is caused by a mutation on chromosome 13 and SCA 10 triggering mutation occurs on chromosome 22. These different SCAs share some clinical features such as impaired gait, dysarthria and oculomotor disturbances of cerebellar genesis. On the other hand, other sings can be helpful to distinguish them, like psychiatric episodes, tremors and cognitive impairments. Nevertheless, there is almost no clinical signs absolutely specific for a single SCA subtype (Schols et al., 2004) and therefore the diagnose is established through the presence of the combination of these symptoms with the aid of genetic tests to assess the presence of a disease-specific mutations.

1.2. Machado-Joseph Disease

Spinocerebellar Ataxia Type 3 (SCA3), commonly known as Machado-Joseph Disease (MJD), is an autosomal dominant inherited progressive neurodegenerative disease caused by an over-repetition of the CAG triplet in the *ATXN3* gene (Matos et al., 2011; Paulson and Fischbeck, 1996). MJD is the most common autosomal dominant ataxia worldwide, showing higher frequencies of incidence in countries like Portugal, Brazil, Singapore, China, Netherlands and Japan. The highest worldwide prevalence occurs in Portugal, in the Flores Island (1/239) (Bettencourt and Lima, 2011) (Figure 1).

Figure 1. Global representation of the prevalence of MJD.

1.2.1. *MJD1* gene and Ataxin-3 protein

The disease locus was mapped in 1993 by Takiyama and collaborators to the long arm of chromosome 14 (14q24.3-q32) (Takiyama et al., 1993) and the increased number of CAG repeats present in the 10th exon of the *ATXN3/MJD1* gene was shown to exist in all the affected individuals, but it was only in 2001 that the gene structure was described (Ichikawa et al., 2001) (Figure 2).

The normal *ATXN3/MJD1* gene usually has 10-51 CAG repeats, while in patients this gene contains 61 to 87 CAG repeats (Maciel et al., 2001). Although, the exact CAG number above which the pathology appears is still in discussion (Gu et al., 2004; Takiyama et al., 1993; van Alfen et al., 2001).

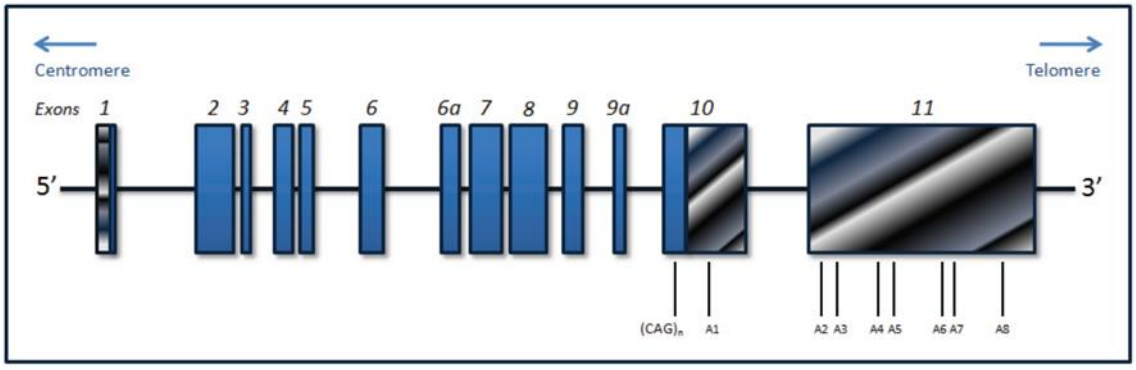

Figure 2. Schematic representation of *ATXN3/MJD1* gene. (Bettencourt and Lima, 2011)

The Ataxin-3 is a ubiquitously expressed protein with 42 kDa and is composed by a globular N-terminal catalytic Josephin domain and a C-terminal tail containing two or three ubiquitin interacting motifs and the polymorphic polyglutamine tract, which is extended in MJD (Matos et al., 2011; Tzvetkov and Breuer, 2007). Although the exact cellular functions of the Ataxin-3 are still not unveiled, it is known that Ataxin-3 is a polyubiquitin-binding protein, with evidences suggesting that this protein plays a major role in the ubiquitin-proteosome system and in the regulation of the transcription. In fact, it was shown that Ataxin-3 protein is involved in the regulation of 290 genes in *C. elegans*, most of them related to cell structure, mobility, signalling and in the Ubiquitin-Proteasome pathway. Thus, Ataxin-3 is thought to contribute to proteasome-mediated protein degradation by binding polyubiquitylated proteins, preferably chains containing four or more ubiquitins which is the chain length required for proteasome degradation (Boeddrich et al., 2006; Burnett et al., 2003). Consequently, contributing to the cellular removal of misfolded and mutated proteins. In fact, several studies demonstrated that interfering with the ubiquitin-proteasome system is possible to improve MJD. In 2013, it was shown that the overexpression of Beclin-1, described as a crucial protein for the autophagy pathway, improved motor coordination, balance and gait in MJD-mice (Nascimento-Ferreira et al., 2013).

1.2.2. Clinical presentation and neuropathology

MJD patients present several motor and non-motor symptoms. Motor symptoms include ataxia, dystonia, ophtalmoplegia and dysarthria (Coutinho and Andrade, 1978), while non-motor symptoms include cognitive impairment and sleep disorders. However, patients very often present a big heterogeneity of symptoms, which lead the clinicians to subcategorize the disease (Paulson, 2007) into 5 subtypes, based mainly on the age of onset, progression and severity of different symptoms like limb and gait ataxia and ophtalmoplegia. Being type 1 MJD the one with the earliest mean age of onset (5-30 years of age) and type 2 the most common with a mean age of onset of 36 years and presenting ataxia, pyramidal deficits and progressive external ophtalmoplegia (Costa Mdo and Paulson, 2012).

MJD-associated brain alterations consist of widespread neuronal degeneration affecting many brain regions such as the cerebellum, brainstem and basal ganglia. Usually there is a marked atrophy of the brainstem, spinal cord and cerebellum and also depigmentation of substantia nigra. Neuronal loss is also found in Clarke's column and anterior horn of the

spinal cord with consequent degeneration of the anterior spinal cord roots and skeletal muscles of the extremities (Durr et al., 1996; Schulz et al., 2010; Yamada et al., 2008).

Mutant Ataxin-3 is aggregated into neuronal intranuclear inclusions and are present both in affected and unaffected regions (Rub et al., 2008), which is a hallmark for MJD (Schols et al., 2004). These intranuclear inclusions are round structures with size varying from 0.7 to 3.7 μm, composed by normal and mutant Ataxin-3 (Paulson et al., 1997), ubiquitin and other proteins like transcription factors and Heat shock proteins. The presence of these aggregates in the cytoplasm (Hayashi et al., 2003) and in axons (Seidel et al., 2010) has also been reported. The impact of these inclusions in the neuropathology is not clear, some reports indicate that the inclusions presence is a cellular response in order to capture the mutated protein and reduce its toxic effect (Cummings et al., 1999; Klement et al., 1998), while other studies suggest that the imprisonment of some cellular components, such as transcription factors, in these aggregates result in severe impairments in cellular function, as transcriptional abnormalities, leading to neuronal degeneration (Yamada et al., 2001).

1.2.3. Pathogenesis and Therapeutic approaches

Although the mutation leading to MJD is well described, the intrinsic mechanisms on the molecular level that lead to the development of the disease is not fully understood and there are many pathogenic mechanisms that can be related to the disease establishment and progression (Figure 3). The most commonly described pathogenic mechanism is the deposition of the mutant Ataxin-3 protein as intranuclear neuronal inclusions that alter cellular functions. This is caused by interactions between the mutant protein and several other proteins, resulting, namely, in the entrapment of the later in the inclusions. This leads to the depletion of Ataxin-3 and other proteins enrolled in the Ubiquitin-proteasome (UPS). As previously stated, the UPS malfunction can lead to the increase of misfolded proteins cellular levels and, the accumulation of these proteins trigger neuronal death. Additionally, autophagy is also disrupted because mutant Ataxin-3 inclusions can sequester proteins of major importance to this mechanism. Other pathogenic mechanisms include the impairment of axonal transport, which might be caused by mutant Ataxin-3 inclusions and calcium homeostasis dysregulation, given that mutant Ataxin-3 has been shown to interact with calcium channels impairing the neuronal communication (Chen et al., 2008).

There is no effective treatment to cure or delay MJD progression; however in the last years different therapeutic approaches have been developed aiming at the targeting of

pathogenic mechanisms described to be involved in MJD, suppressing some symptoms and ameliorating the disease.

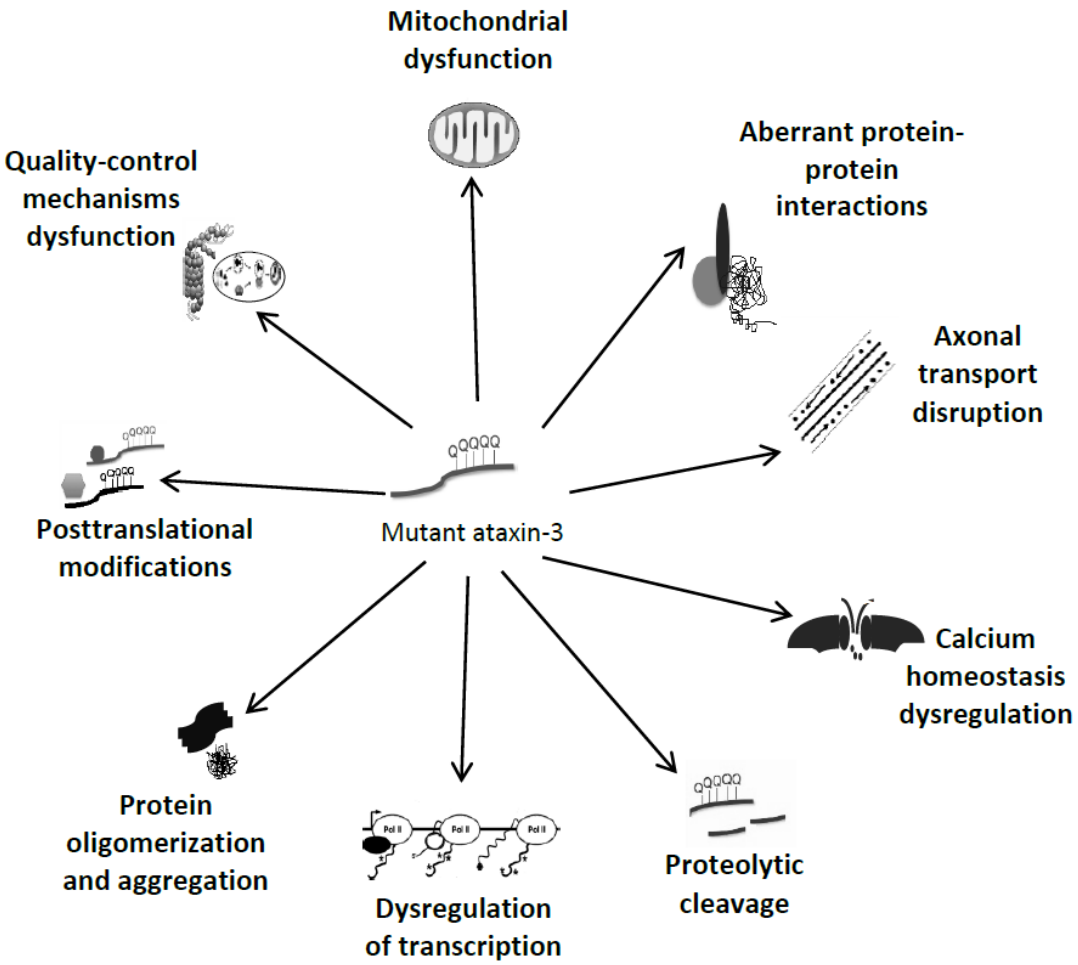

Figure 3. ***Mechanisms of pathogenesis in MJD. (Nóbrega and Almeida, 2012)***

1.2.3.1. RNA interference (RNAi)

The most direct solution to interfere with the pathogenesis triggered by the mutant Ataxin-3 is to reduce the expression of the mutant *ATXN3* mRNA. RNA interference (RNAi) is a process found in most eukaryotic cells by which gene expression is inhibited. This RNAi pathway are guided by small RNA molecules, microRNA or small interfering RNA that are derived from hairpin RNA structures encoded in the genome or synthetic molecules introduced into cells (Kim et al. 2007). These effectors (siRNA and miRNA) induce gene silencing by either inducing cleavage of the complementary mRNA or by simply repressing

mRNA translation. Naturally, RNAi pathway is an important intrinsic immunity defence mechanism against viral infection and is also extremely important during development, where it regulates gene expression, mainly through miRNA different expression levels at different timings to regulate morphogenesis. Since its discovery RNAi has been used in many areas such as medicine, biotechnology and experimental biology. This practical tool allow to manipulate the genome in order perform gene knockdown suppressing specific genes of interest to access its cellular and physiological roles. RNA interference is a technique that has been shown to be effective in downregulating gene expression and rescue phenotype in neurodegenerative disorders such as HD, SCA1 and SCA3 (Alves et al., 2008a; Lombardi et al., 2009; Xia et al., 2004) .

1.2.3.2. ShRNA

ShRNAs are artificial double stranded RNA molecules with a hairpin turn that have been used to silence specific genes, by impairing their expression, via RNAi. ShRNAs are synthesized in the nucleus of cells forming a hairpin-like structure consisting of two complementary RNA sequences linked by a short loop. After transcription, shRNA are processed by Drosha and then are exported to the cytoplasm by exportin-5. In the cytoplasm the loop is cleaved by DICER, forming a double stranded small interfering RNA (siRNA), which is then loaded into the RNA-induced silencing complex (RISC). Then, one of the strands is eliminated and the complex is directed by the guiding strand to the complementary mRNA molecule inhibiting its transcription or triggering the degradation of the target mRNA (Moore et al., 2010), (Figure 4).

In the particular case of MJD the major problem in the implementation of RNAi to mutant Ataxin-3 gene silencing could be to guarantee the specific silencing of the mutant allele without interfering with the wild type Ataxin-3 levels, since the silencing of the normal allele might be harmful. To overcome this problem, in our lab it has been successfully targeted mutant Ataxin-3 while preserving wild-type Ataxin-3 both *in vitro* and *in vivo* via a shRNA mediated silencing that was designed to specifically target a single nucleotide polymorphism present in more than 70% of patients (Alves et al., 2008a). This shRNA have been delivered by lentiviral vectors and allowed a safe and robust down-regulation of mutant Ataxin-3 levels in MJD cellular and mouse models.

1.2.3.3. Increasing misfolded proteins clearing, preventing mutant Ataxin-3 aggregation and fragmentation

Accelerating the proteolysis mechanisms could also be an effective way to delay the progression of MJD, since, as previously described, in MJD there is accumulation of misfolded proteins resulting from the autophagy and UPS dysregulation. Increasing the ubiquitin-proteasome system related factors will increase ubiquitination and increase the rate of protein degradation, thus reducing protein aggregation and possibly reducing cell death. This hypothesis was confirmed in 2005 where it was shown that ubiquitin ligase CHIP (C-terminus of Hsc70-interacting protein) reduces aggregation and promotes degradation of polyQ proteins (Jana et al., 2005; Miller et al., 2005). As well as the up-regulation of autophagy by inhibiting mTOR pathway, using rapamycin, in a mouse model of SCA3, resulted in selective clearance of mutant Ataxin-3, decreasing the number of aggregates and soluble Ataxin-3, while the normal protein was not affected, alleviating MJD pathogenesis and improving motor coordination in MJD mouse models (Menzies et al., 2010; Nascimento-Ferreira et al., 2011).

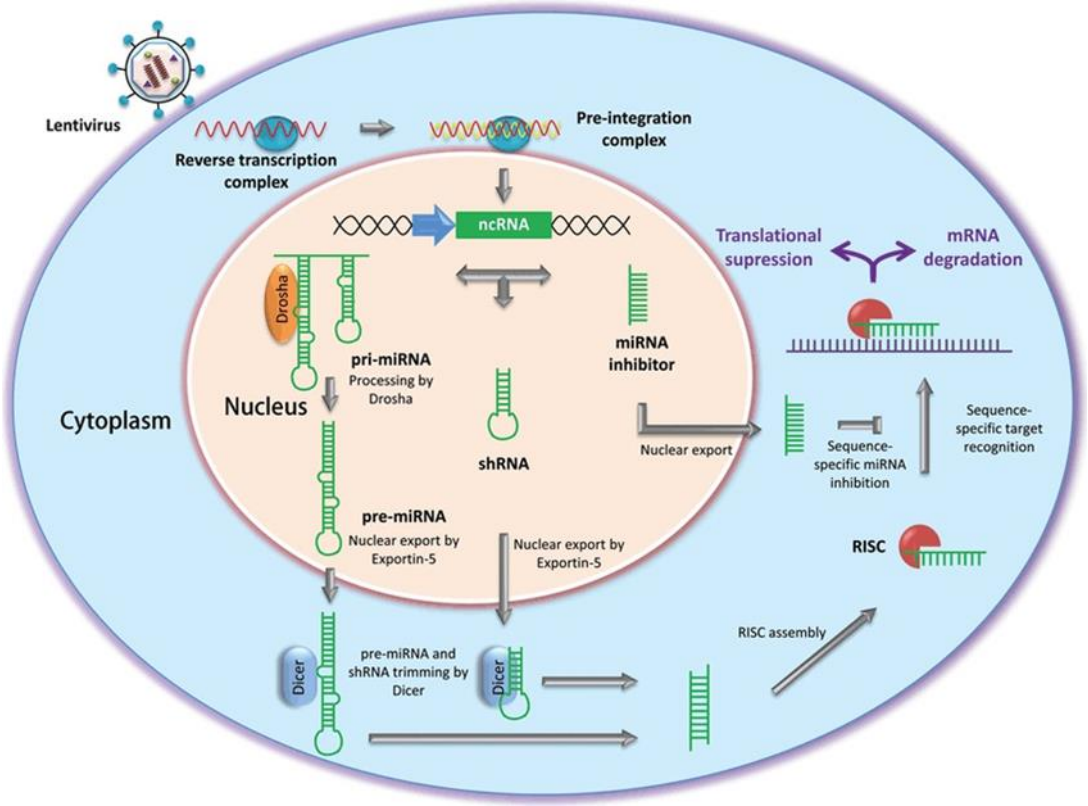

Figure 4. Lentiviral delivery of small non-coding RNAs, namely miRNA, shRNA and miRNA inhibitors, and mechanism of action. (Primo et al., 2012)

Preventing the aggregation and oligomerization has also been the research target of different research groups and several compounds, such as Congo red, thioflavine S, chrysamine G, Direct fast yellow and even engineered antibodies, have already been shown

to act has potential inhibitors of polyglutamine protein aggregation in HD ((Heiser et al., 2000; Wolfgang et al., 2005). Small peptides or molecules, like the ubiquitin ligase CHIP or calpain inhibitor BDA-410 have also been used to modulate protein folding and stabilize proteins in their native conformation preventing aggregation, namely in MJD (Jana et al., 2005; Simoes et al., 2014).

The fragments of mutant Ataxin-3 have been associated to neurotoxicity (Boeddrich et al., 2006). Therefore, the impairment of mutant Ataxin-3 fragments production by blocking proteases involved in Ataxin-3 cleavage, using calpastatin overexpression to inhibit calpain activity, is a strategy that has been explored as a therapeutic approach for MJD treatment (Simoes et al., 2012). Similar approaches have been used in other neurodegenerative diseases like AD or HD, where mutant protein fragments contribute to neurotoxicity (Citron, 2004; Gafni et al., 2004).

1.2.3.4. Reversion of transcription downregulation, calcium homeostasis stabilization and neuroprotection

Transcription might also be a target for therapy in polyglutamine-extended proteins. In SCA3, has been shown that mutant Ataxin-3 represses transcription and this transcriptional dysregulation has been thought to play an important role in the neurodegenerative mechanisms of PolyQ disorders (Chou et al., 2008). The reversion of transcriptional downregulation present in a MJD mouse model delayed the onset of symptoms and increased the survival rate of those mice. Chou and colleagues used sodium butyrate as HDAC (Histone deacetylase) inhibitor reverting translational repression induced by mutant Ataxin-3. Alternatively, Nobrega and colleagues showed that restoring Ataxin-2 levels through its overexpression in MJD mice, reduced mutant Ataxin-3 levels (Chou et al., 2011; Nobrega et al., 2015).

Since calcium signalling is affected and thought to play an important role in MJD pathology and, as mutant Ataxin-3 has been shown to activate intracellular calcium channels leading to an unbalance intracellular calcium homeostasis. Calcium stabilizers, such as Dantrolene, can be considered as therapeutic approaches and were already shown to improve motor performance and prevent neuronal loss in MJD-transgenic mice (Chen et al., 2008).

Administration of molecules with neuroprotective properties has been also explored. Some groups have used neurotrophic factors for therapy of PolyQ diseases (de Almeida et

al., 2001), for example in HD the BDNF (Brain-derived neurotrophic factor) administration, which is diminished in the disease, was shown to be effective in preventing neuronal loss and motor dysfunction (Xie et al., 2010).

Thus, there are several different therapeutic strategies with potential to mitigate the neuropathology process triggered by mutant Ataxin-3 and improve MJD-associated neuropathology and motor impairments. Nevertheless, by the time of diagnose most of the patients already display an extensive neuronal loss. Therefore, we speculate that to induce a complete recovery of the disease cell-based therapies will be needed, either used alone or in combination with other therapies.

2. Cell Therapy

Cell therapy consists on the use of cells or cell-based products in order to replace death or defective cells with the purpose to restore the tissue or organ functions lost in the disease or trauma process (Kim and de Vellis, 2009; Lindvall et al., 2004). Stem cells are some of the more promising cells to be use in the field of cell therapy, given their ability of proliferation, migration and differentiation into the needed type of cells in order to regenerate the affected tissues.

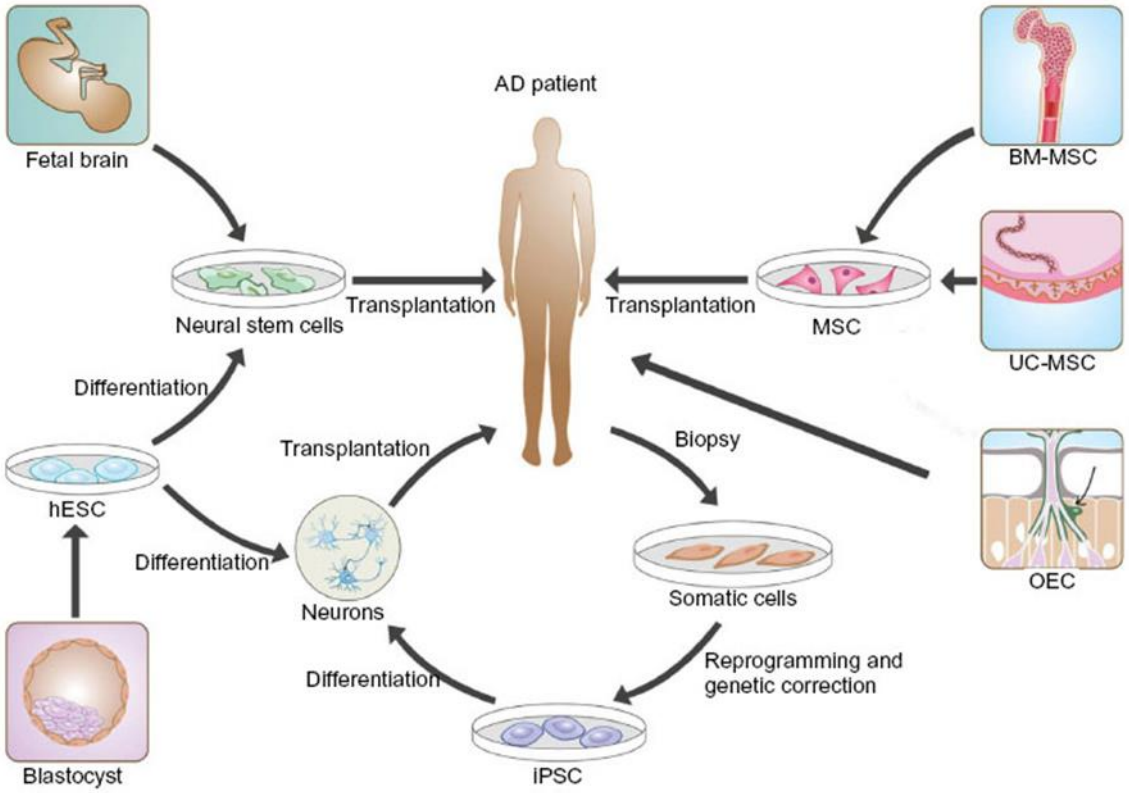

Figure 5. ***Different sources of Stem cells for cell therapy. (Han et al., 2014)***

There are different types of stem cells prone to be used in cell therapy. Namely, pluripotent stem cells, like the embryonic stem cells (ESCs), obtained from embryos from the inner cell mass of the blastocyst; multipotent stem cells like mesemchymal stromal cells present in bone marrow and adipose tissue and, neural stem cells that can be isolated from the nervous system in different stages of development, namely fetal and adult neural stem cells (Kim and de Vellis, 2009). More recently, the discovery that is possible to induce mature adult cells, like fibroblasts, to revert into a pluripotent stage, into the so-called induced pluripotent stem cells (iPSC) (Figure 5) has revolutionized the field of stem-cell therapy (Alison et al., 2000; Bernardo et al., 2009; Rippon and Bishop, 2004; Takahashi and Yamanaka, 2006), namely of personalized cell-based therapies.

All of these different stem cells have different properties and have been used as cell sources for cell therapy in very different diseases. Several pre-clinical studies have shown cell therapy using stem cells to be effective in the treatment of some neurodegenerative disorders such as MJD (Mendonça et al 2015), HD (Dunnett et al., 1998; Johann et al., 2007) and PD (Wernig et al., 2008). Importantly, some clinical trials have also demonstrated the great potential of these therapies in diseases like Parkinson's (Li et al., 2016; Olanow et al., 2003) and Huntington's (Freeman et al., 2000).

In the field of human brain stem cells transplantation for neurodegenerative diseases treatment, the research done in the last three decades in Lund University illustrates the big efforts made in this field and the promising results obtained with stem cells. The first clinical trials for cell transplant into the brain of Parkinson's disease patients consisted of fetal-derived dopamine neuroblasts transplantation into the putamen of the patients' brain. The first two patients to undergo this procedure were operated in 1987 and although these two transplants showed minimal effects and no real proof of graft survival (Lindvall et al., 1989), in the next year the procedure was repeated with some adjustments. This time in the third and fourth patients the results were promising, showing motor improvement in the limb contralateral from the grafts and the clinical improvements showed to persist 10 years after transplantation (Piccini et al., 1999). Since these first transplants, over the last three decades, 18 patients were submitted to the procedure, showing heterogeneous but very encouraging results (Bjorklund and Lindvall, 2017). Recently one of the first patients died 24 years after transplantation, from reasons unrelated to the transplant, and the postmortem histopathological analysis showed that graft-derived dopaminergic reinnervation of the putamen was maintained for 24 years after transplantation (Li et al., 2016).

Despite these very promising results, there are issues hampering research in this field. One major problem is related to the origin of the human stem cells to be used in

transplantation, mainly in the case of human ESCs and fetal stem cells. As opposed to adult stem cells and iPSC, ESCs and fetal stem cells raise ethical problems, since ESCs require the destruction of human embryos to obtain cells form the blastocyst and the fetal stem cells implicate the use post-abortion fetal tissue, which is involved in ethical and political controversy. These are long discussed issues and there is obviously some discordance in the matter regarding the use of human ESCs mainly due to difference of opinions in the long discussion of where life begins. In a more religious point of view, life begins at conception and so the embryo is a person and must be respected and preserved. On the other hand some people believe that the embryo becomes a person at a later stage in development, accepting its use for research and clinical purpose under certain specific situations (Lo and Parham, 2009; Mendonca et al., 2018), namely the use of surplus frozen embryos that remain after the *in vitro* fertilization program has been finished.

Other important limitation is the immune rejection observed with grafts obtained from donors, the allogenic transplantation has the additional disadvantage of requiring the use of immunosuppressive drugs that are associated to significant adverse effects (Mendonca et al., 2018).

Thus, these problems galvanized the stem cell research field in order to get alternative cell sources, which resulted in induced pluripotent cells (iPSCs) discover that besides evading the ethical and moral problems also evade the immunological problems because it allows the production of the type of cells required for transplantation from the cells of the patient to be treated.

Besides being used as cell sources for therapeutic applications, these cells also allowed the development of new cellular models to replace or reduce the use of animals in research. Not only in cell therapy but also in other research fields, animals are modified to serve as models for scientific research. These models, however, are not completely reliable and some results cannot be translated to humans. Even though there are some conserved pathways between species, namely between humans and the animal models, which in their majority are rodents, there are also large genetic differences and gene regulation that lead to large physiological differences. Not only the differences between the models and humans are important, but also variations within specific species or between close species that are used as models. This leads to some reports of results in a specific model that cannot be replicated in another model. It is, therefore, important to understand that a specific model is not always able to mimic a specific human disease, that even in humans its symptoms vary from patient to patient. (Barre-Sinoussi and Montagutelli, 2015). Moreover, no rodent brain can replicate the complexity of human brain and, therefore studies of human stem cells transplantation for

neuroregeneration evaluation performed in rodents´ brains will inevitably be drastically limited by these inter-species differences. Thus, as iPSC technology allow the development of different types of cells it is now possible to generate human cell models for diseases lacking effective models, such as human organoids (Bershteyn et al., 2017; Fatehullah et al., 2016; Mendonca et al., 2018).

2.1. Understanding the mechanism of stem cells transplantation promoted recovery

Even with many positive results obtained in many studies regarding cell therapy, most of the time, the mechanisms behind such results, as well as the types of cells promoting it, are not fully understood. Nevertheless, it has been described that the transplanted cells improve disease symptoms through the integration of new cells derived from the graft, provide trophic support to endogenous cells or trigger immunomodulation (Pluchino et al., 2005; Steinbeck and Studer, 2015; Xu et al., 2011).

Thus, one proposed mechanism is the functional integration of the graft-derived neurons into the neuronal network of the host's brain. This mechanism can potentially fully repair the damaged area and rescue behavioural impairments. It has been suggested in different studies that the observed behavioural recovery is in part a result of the establishment of new synaptic connections between the brain and the graft (Clarke and Dunnett, 1993). Concerning to the trophic support mechanism, it has been described that grafted cells are capable of increasing the survival and recovery of the host neurons by secreting neurotrophic factors like BDNF, NGF (Nerve growth factor) and GDNF (Glial cell-derived neurotrophic factor) (Bohn et al., 1987; Wang et al., 2013; Xu et al., 2011; Xu et al., 2013), and this mechanism can be used to target specific diseases that lack certain factors, by genetically modifying cells to overexpress the needed factors, for example the use of BDNF-secreting stem cells in Parkinson's disease (Somoza et al., 2010). Finally, other mechanism that have been associated to the positive modulation resulting from stem cells brain transplantation is triggered by the cross-talk between transplanted stem cells and the immune system (Kokaia et al., 2012). In fact, some studies demonstrated that transplanted stem cells decrease neuroinflammation, reducing neuronal death. The work of Pluchino and colleagues, provided evidence that replacement of the affected or death cells might not be necessarily the main mechanism behind the observed recovery upon stem cells transplantation and, it is instead the immune regulation that is the main putative mechanism in the observed improvement of a Multiple Sclerosis model (Pluchino et al., 2005; Pluchino

et al., 2009). Additionally, the transplanted stem cells can also promote successful functional myelination of axons and lead to locomotor recovery and thus might be used in the treatment of dysmyelinating diseases (Faulkner and Keirstead, 2005; Uchida et al., 2012).

In summary, several mechanisms have been described to explain the positive effects resulting from transplantation of stem cells. Also it is probable that not only one of these mechanisms is responsible for the observed effects, probably the observed outcomes result from a combination of different effects. Finally, it is also important to understand which cell type produce the observed effects, since transplanted stem cells may differentiate into different types of cells (Steinbeck and Studer, 2015).

2.2. Induced pluripotent stem cells

Human stem cell research is a relatively new and promising field of research. Although its progress has been hampered mainly due to ethical problems concerning to the origin of embryonic stem cells (ESCs) and the need to destroy human embryos to establish the cell lines. This led to the search for alternatives and in 2006, Yamanaka and collaborators have showed for the first time that the expression of certain genes could revert adult mature cells into pluripotent stem cells (Takahashi and Yamanaka, 2006). Mature cells were successfully induced back to a pluripotent stage by forcing the cells to express four transcription factors: SOX2, OCT4, KLF4 and c-Myc. These cells, designated as induced pluripotent stem cells (iPSCs) are very similar to ESCs, ie, these cells are pluripotent, have self-renewal ability and have the potential to originate all tissue types of an organism (Figure 6). Thus, the main advantage of iPSCs is that these cells are not associated to ethical and moral controversies, as compared to ESCs (Meyer, 2008). Moreover, theoretically, iPSCs can also overcome immunological rejection problems, because it is possible to generate patient-specific cells (Vitale et al., 2011).

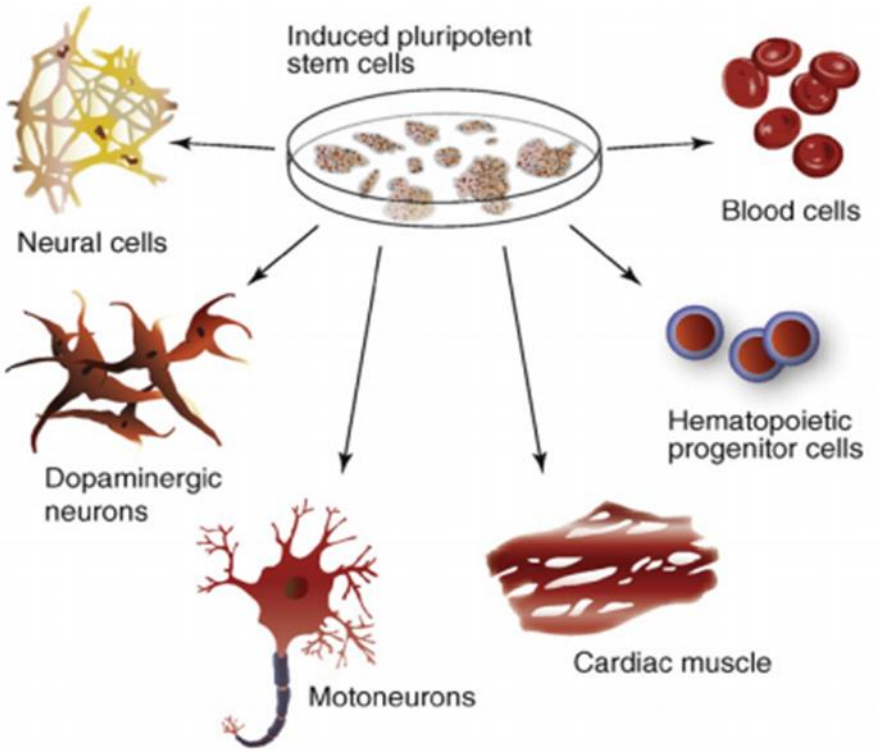

Figure 6. ***iPSCs differentiation into different types of cells (Amabile and Meissner, 2009).***

iPSCs came to revolutionize the stem cell research field and were quickly implemented in many research areas. Namely, iPSCs have been used in drug discovery and developmental studies, as well as for modelling various diseases and have been tested in cell replacement therapeutic strategies.

2.2.1. Cell Reprogramming

Induced Pluripotent Stem Cells are generated by the expression of specific transcription factors that force mature cells into a pluripotent stage. This can be done using different factors and different gene delivery tools, such as integrating vectors, excisable-integrating vectors and non-integrating vectors (Shao and Wu, 2010), which result in different rates of efficiency and safety. The reprogramming efficiency is highly dependent on which type of cells the reprogramming is performed and, different somatic cells require different factors. Multipotent stem cells are easier to be induced into pluripotent cells as compared to differentiated cells. For example, mouse adult neural stem cells were converted using only Oct4 and Klf4 (Kim et al., 2008) and Oct4 and Sox2 were shown to be enough to reprogram human cord blood stem cells into iPSCs (Giorgetti et al., 2009).

2.2.1.1. Integrating vectors

Concerning integrating vectors, retrovirus is the most common choice due to their high transduction efficiency. These are called integrating vectors since, after delivery, the viral genome is integrated into the DNA of the cells and begins to be transcribed and expressed. Thus, the genetic information for the reprograming factors become virtually permanent and these genes are passed to the progeny (Shao and Wu, 2010).

In Yamanaka and colleagues' work was implemented this type of vectors, a Moloney murine leukaemia virus-based vector in which the transgenes were controlled by a promoter that is silenced in pluripotent stem cells. Thus, as expected, the reprogramming factors were silenced in the newly formed iPSC, which is a strategy to increase the safety of the system, by shutting-down genes related to cancer, such as *c-Myc*. Although, there are reports indicating that the promoter can be re-activated, triggering the expression of c-Myc in differentiated cells and causing tumors formation.

Lentivirus is a subclass of retrovirus that is widely used in our group, namely to perform cell reprogramming. The main advantage of lentivirus usage is the capacity to infect dividing and non-dividing cells, contrary to the retroviruses that only infect dividing cells. Moreover, similarly to other retroviruses, after lentiviral infection occurs the inclusion of the viral genome in the host genome. One possible drawback of using lentiviral vectos, as well as other integrating vectors, is the unpredictability of the integration site of the viral DNA, which when inserted in certain points can lead to dysfunction of genes or even induce activation of oncogenes resulting in tumorigenicity.

2.2.1.2. Excisable integrating vectors

Integrating vectors are more efficient as compared to non-integrating, nevertheless, the potential tumor induction with these vectors resulted in the exploitation of excisable integrating vectors techniques. One example is piggyBac transposons, which are mobile genetic units that move from one place to another within the cell's genome. Class 1 transposons are first transcribed to RNA, and then are reverse transcribed to DNA being finally inserted into another position in the genome. While Class 2 transposons, like the piggybac transposon, are mobile genetic elements that are excised by a transposase and are then inserted into another region of the genome (Shao and Wu, 2010). The use of this type of transposons has already been documented, after reprogramming, the ectopic expression of transposase leads to excision of the transposons without being inserted into

other regions leading thus to elimination of the reprogramming factors (Kaji et al., 2009; Woltjen et al., 2009). Although the many advantages of this approach, the use of this system on hard-to-reprogram cells is still to be demonstrated, and also transpositions are not always precise and can leave footprints in the generated iPSC (Wang et al., 2008).

2.2.1.3. Non-integrating vectors

As the name suggests these vectors do not integrate the genetic information of the reprogramming factors in the genome of the cells. This approach was developed in order to avoid some downsides of integrating vectors, namely the possible spontaneous reactivation of the integrated transcription factors or to avoid the genomic modification done by the random gene integration, namely the activation of oncogenes or the silencing of important genes.

In Yamanaka's group, a strategy to generate iPSCs from mouse embryonic fibroblasts without the integration of reprogramming factors was established by using circular plasmids expressing the reprogramming factors (Okita et al., 2008). The generated iPSCs were similar to ESCs; nevertheless, the efficiency of reprogramming by these plasmids was much lower as compared to integrating vectors. Also, using this approach, multiple rounds of transfection are needed, since the plasmids only stay in cells for a few days (Gonzalez et al., 2009; Okita et al., 2008). Therefore, episomal plasmids carrying viral elements were tested. The viral elements introduced allow them to replicate once per cycle and this mechanism ensures the retention of the vectors over various cell division cycles. The rate of loss of these vectors is low enough to guarantee that they remain in the cells long enough for the reprogramming to occur, needing only one transfection. On the other hand, the vectors are eventually lost overtime, therefore they end up not being present in the derived iPSCs. This method has shown to have approximately the same efficiency levels of the integrating vectors (Nanbo et al., 2007; Yu et al., 2009).

Another technique of non-integrating vectors involves the delivery of reprogramming factors via adenovirus infection, which are non-integrative viruses, but this approach was shown to have the same low efficiency as the plasmid-mediated reprogramming. In fact, in Yamanaka's group, they first tried to use different adenoviral vectors for reprogramming factors delivery and failed to produce iPSC, probably due to inability to express all the factors into the same cells (Okita et al., 2008). Later, it was shown to be possible to reprogram human fibroblasts to iPSCs using adenovirus vectors containing the four transcription factors. Nevertheless, although the expression level of these genes in the

infected cells was much higher than by using retroviral/lentiviral vectors, the reprogramming efficiency was extremely low (Zhou and Freed, 2009).

Other cell reprogramming strategies include the delivery of proteins or mRNA of the reprogramming factors onto the cells instead of delivering DNA. Recombinant proteins were generated by adding a poly-arginine protein transduction domain to the C-terminus of the four reprogramming factors, Oct4, Sox2, Klf4 and c-Myc, allowing these proteins to cross biologic membranes and entering into the cell´s nucleus (Kim et al., 2009; Zhou et al., 2009). mRNAs were also synthesized via *in vitro* transcription and a KMOSL cocktail (consisting of five reprograming factors: KLF4, c-MYC, OCT4, SOX2 and LIN28) were transfected into cells using a cationic vehicle. This approach using mRNA was shown to have surprisingly higher reprogramming efficiency than the virus approach (Warren et al., 2010).

2.2.2. Small molecules for Chemical induced pluripotent stem cells

As previously stated, after the emergence of iPSCs, initially reprogramed from mature, differentiated cells, some drawbacks came to light. Since these were initially reprogrammed using viral vectors such as lentivirus, the main concern that arose was the integration of the transgenes into the genome of the cells, potentially leading to undesired effects. Thus, it was readily hypothesized that alternatives to the use of viral-based strategies could be developed.

Besides the already mentioned non-integrating vectors and excisable vectors, another potentially safer alternative based on the use of small chemical molecules to mimic the cell-reprograming molecular changes induced by the expression of the four factors needed to obtain the iPSCs has been explored (Ichida et al., 2009; Shi et al., 2008a; Zhu et al., 2010).

These small molecules are compounds able to modulate cellular mechanisms that are altered during cellular reprograming such as modulation of cell signalling and gene expression through induction of epigenetic changes. This chemical approach would bring some advantages when compared to genetic manipulation. Besides the aforementioned avoidance of transgene (oncogenes) integration in the genome, it is also an approach that is easier and cheaper to implement and use. Additionally, it allows a better control of the concentrations to which the cells are submitted and it is much easier to cease the effect of these molecules, as compared to other strategies (Biswas and Jiang, 2016).

This chemical induction consists mainly in the use of compounds that differentially modulate epigenetic alterations to modify gene expression. Here we have small molecules

that modulate histone acetylation as well as DNA and histone methylation. Briefly, DNA methylation is responsible for silencing genes, once a methyl group is added to the DNA it blocks the binding of a transcription factor thus inhibiting the initiation of transcription. Histone acetylation leads to chromatin condensation resulting in silencing of certain genes. As well as histone acetylation, histone methylation is also highly controlled and also influences chromatin condensation; alterations that lead to differently expressed genes (Biswas and Jiang, 2016; Jung et al., 2014).

The ultimate goal of achieving complete reprograming to iPSCs only using chemical compounds has been pursued by several groups. Huangfu and colleagues, in 2008, (Huangfu et al., 2008) showed that by introducing a histone deacetylase inhibitor allow to perform the reprogramming with only two of the Yamanaka´s reprogramming factors. In fact, they demonstrated that the use of valproic acid with SOX2 and Oct 3/4 expression (without c-Myc and Klf4) lead to the generation of iPSCs; additionally they showed that this strategy has a much higher reprogramming efficiency. This was the first time it was reported the generation of iPSCs with the aid of small molecules, but was quickly followed by other studies using other molecules, although always with the need of genetic manipulation to express one or more of the reprogramming factors. For example, Shi and colleagues (Shi et al., 2008b) were capable of reprograming mouse embryonic fibroblasts by expressing Oct4 and Klf4, in combination with two small molecules, BIX-01294 (histone methytrasferase inhibitor) and BayK8644 (calcium channel agonist). Finally in 2013, Hou and colleagues (Hou et al., 2013) reported the generation of mouse iPSCs using only small molecules. Previously, they have successfully reprogrammed cells expressing only Oct-4 (in combination with VPA, CHIR99021, 616452 and Tranylcypromine). Thus, they further worked on the identification of other compounds that could replace Oct-4 and enable cell reprogramming in its absence. After screening several molecules they identified Forskolin (FSK), 2-methyl-5-hydroxytryptamine (2-Me5HT), and D4476 as Oct-4 substitutes. Thus, in combination with the previous identified cocktail that enabled reprogramming with Oct-4 ("VC6T" - VPA, CHIR99021, 616452 and Tranylcypromine) they reached the final cocktail of 7 small molecules to obtain iPSCs (VPA, CHIR99021, 616452, Tranylcypromine, Forskolin (FSK), 2-methyl-5-hydroxytryptamine (2-Me5HT), and D4476). .

Thus, there are several reports using a variety of combinations of small molecules either to increase the reprogramming efficiency of the four reprogramming factors, or to generate iPSCs without gene manipulation (Li et al., 2011; Yuan et al., 2011; Zhu et al., 2010).

2.2.3. Direct Reprogramming

Direct reprogramming, also called “transdifferentiation“, is the conversion of one type of differentiated cell directly to another without going through a pluripotent stage. In 2010, Vierbuchen and colleagues (Vierbuchen et al., 2010), successfully reprogrammed mouse embryonic and postnatal fibroblasts directly to neurons by forcing the expression of Ascl1, Brn2, and Myt1l (neuronal transcription factors), to which they called induced neurons (iNs). Later, Hu and colleagues (Hu et al., 2015) performed this with human fibroblasts using a cocktail of 7 small molecules (VPA, CHIR99021, Repsox, Forskolin, SP600125, GO6983, and Y-27632). Moreover, Zhang and colleagues (Zhang et al., 2015) demonstrated that adult astrocytes could be directly reprogrammed into functional neurons with a mixture of 9 small molecules (LDN193189, SB431542, TTNPB, Tzv, CHIR99021, VPA, DAPT, SAG, and purmorphamine).

Importantly, the fact that through this process of transdifferentiation, the cells bypass the pluripotent stage led to the hypothesis that these iNs would maintain some characteristics of the “original” cell, mainly regarding epigenetics and aging markers. So, it was demonstrated that iNs maintain the age-specific transcriptional profile consistent with the donor cells, specifically the decrease in a nuclear transport receptor impairing nucleocytoplasmic compartmentalization. As opposed to these iNs, iPSC-derived neurons did not retain the aging associated gene signatures, as iPSC restored nucleocytoplasmic compartmentalization in aged cells. (Mertens et al., 2015). Huh and colleagues reached the same conclusion relatively to the “epigenetic clock”. They accessed age-associated DNA methylation profiles and observed a reset in these profiles with the iPSCs reprogramming. (Huh et al., 2016)

These differences are important to have in mind when deciding for one of the strategies. iNs retain age-associated characteristics from fibroblasts to neurons; thus, they might be a better alternative for modelling diseases associated with aging as opposed to iPSCs that might be a better choice to study developmental diseases (Drouin-Ouellet et al., 2017) or to be used as a cell source for cell-based therapies.

2.3. Neural Induction

iPSC have the capacity to generate all the types of cells that constitutes an organism. Thus, the next step is to induce these cells into the type of cells needed. This induction process consists of exposing the pluripotent stem cells (PSCs) to specific conditions that will

convert pluripotent into multipotent cells and compromise them in the germ layer of the cells of interest. The culture medium composition and the timing of exposure to define components will dictate the success of the cellular induction. Many different protocols have been established to accomplish this goal, but many of these usually consist in the formation of embryoid bodies before exposing the cells to the factors that will guide them to the desired lineage (ectoderm, mesoderm or endoderm) (Itskovitz-Eldor et al., 2000).

Initially it was described that PSCs show a natural tendency towards neural differentiation as, by removing the self-renewing conditions led to the formation of neural cells, although with low purity (Tropepe et al., 2001). More recently, new protocols have been developed consisting on the modulation of signals that are known to regulate neural induction *in vivo*, being one of these strategies the so-called "dual SMAD inhibition" consisting on the blockage of BMP (Bone morphogenic protein) and TGFβ (Transforming growth factor beta)-signalling driving PSCs to neuroepithelial cells (Chambers et al., 2009).

In another example, Reinhardt and colleagues generated neuroepithelial stem cells through human "embryoid bodies" formation, mainly by submitting them to the combination of the Wnt and SHH (Sonic hedgehog) signalling with CHIR-99021 and purmorpham (PMA). NESCs are multipotent stem cells compromised to the nervous system and can be differentiated simply by removing the supplements that maintain the "stemness", CHIR-99021 and purmorphamine (PMA), originating heterogeneous cultures composed by neurons, astrocytes and oligodendrocytes. More specific cultures are possible to obtain by performing differentiation with supplements specific of the desired cell type, for example astrocytes or peripheral nervous system neurons (Reinhardt et al., 2013).

2.4. Neuroepithelial stem cells

In 2009, Phillip Koch and colleagues derived long-term self-renewing neuroepithelial-like stem cells, to which we will refer to as neuroepithelial stem cells (NESC), from embryonic stem cells. These cells were obtained by differentiation of embryoid bodies to neural rosettes, that within 10 days developed into neural-tube like structure, which are then mechanically isolated and further propagated as free-floating neurospheres (Koch et al., 2009). Anne Falk and colleagues continued this line of work by exploring the use of iPSCs to obtain this type of cells. They demonstrated that regardless of their origin, ESCs or iPSCs (obtained from different sources, either mesenchymal or neural cells), NESC present very promising results (Falk et al., 2012).

NESC were shown to have strong self-renewal capacity and expansion at a scale sufficient for therapy (Poppe et al., 2018). These cells were also shown to be capable of differentiating to neural cell types, such as beta III-tubulin and MAP2 positive neurons and also differentiate in GFAP positive astrocytes. Further tests demonstrated that NESC were capable of generating electrophysiologically functional and synaptically connected neurons *in vitro*, making them a good candidate to be used as *in vitro* models and as a source of cells for cell replacement therapies (Falk et al., 2012).

Thus, aside from the *in vitro* evaluation of NESC, *in vivo* studies were also performed to evaluate its potential for brain transplantation. In these studies, NESC exhibited long-term survival and functional integration into the host's brain of adult rodents (Steinbeck et al., 2012). Importantly, these cells showed different fate after transplantation depending on the site of transplantation, showing site-specific axonal projections, being capable of mimicking different endogenous projections depending on the transplantation site, namely when transplanted into dentate gyrus or in the motor cortex (Doerr et al., 2017; Steinbeck et al., 2012). All these results regarding *in vitro* and *in vivo* differentiation, survival, axonal outgrowth and formation of functional synapsis, make these cells a promising cell source for disease modelling and cell therapy strategies.

3. Objectives

Given the promising potential of stem cell-based neuroregenerative therapeutic strategies in neurodegenerative diseases, the present study aimed at assessing the potential of human induced pluripotent stem cells (iPSCs)-derived neuroepithelial stem cells (NESCs) as a cell source to be use in cell replacement and neuroprotective strategies in neurodegenerative disorders such as MJD.

Therefore, NESCs obtained from neural induction of iPSCs reprogrammed from human fibroblast of both control and MJD patients were extensively characterized *in vitro*. It was studied the potential of these NESCs to give rise to neurons and glial cells upon differentiation. Additionally, neurons functionality was vastly assessed through single cell calcium imaging, and neurite length and functional synapse assessments. The cells were further tested for their potential use as a source of stem cells for brain transplantation. Thus, NESCs were transplanted into the cerebellum of adult NOD.scid mice and the survival, migration, differentiation upon transplantation were evaluated. Finally, it was also evaluated whether there is immune rejection and whether the transplantation of these cells trigger neuroinflammation.

Chapter II - Methods

Cell Culture

Human iPSC-derived NESC, established in our lab, obtained by reprogramming fibroblasts of Control (1 clone/cell line) and MJD-patients (3 clones/cell lines), with lentivirus encoding for Oct-4, Klf4, c-Myc and Sox-2 into iPSC, which were induced to NESC (Reinhardt et al., 2013) were used. These NESCs were maintained on Matrigel-coated (Corning) cell culture flasks in N2B27 medium [DMEM-F12/Neurobasal (50:50) with 1:100 B27 supplement without Vitamin A (Gibco), 1:200 N2 supplement (Gibco), 1% Penicillin/Streptomycin (Invitrogen), 2 mM L-glutamine (Invitrogen)], supplemented with 150 µM Ascorbic acid (Sigma-Aldrich), 3 µM CHIR 99021 (Axon Medchem) and 0.75 µM purmorphamine (Enzo).

Cells were grown in monolayers; for splitting, cells were detached with pre-warmed Accutase (StemCell Technologies) for 5 minutes at 37ºC, diluted in DMEM Knockout for centrifugation at 1100 RPM for 5 minutes.

For cell differentiation, cells were plated on matrigel-coated plates in N2B27medium, supplemented with 0.25 µM Dibutyryl cyclic-AMP sodium salt (dbcAMP, Sigma-Aldrich), 5 µM Forskolin (Sigma-Aldrich) and 2 µM retinoic acid, maintained for 3 weeks, changing medium every three days.

NESCs infection with lentivirus encoding for GFP

The lentiviral vectors encoding for green fluorescent protein (GFP, SIN-PGK-GFP-WHV) were produced in 293T HEK cells using a four-plasmid system as described previously (Alves et al., 2008b; de Almeida et al., 2001). NESCs were transduced with lentiviral vectors encoding GFP. Cells were collected by centrifugation and $3x10^6$ cells were cultured in a T75 flask. Then lentiviral vectors encoding GFP were added to the cells. Twenty-four hours later half of culture medium was replaced to dilute the viruses and on the second day the lentiviral vectors were removed by changing the medium. Cells were submitted to a maturation protocol with BDNF (Peprotech), GDNF (Peprotech), TGF-β 3 (Peprotech), ascorbic acid and dbcAMP (Sigma Aldrich) before transplantation.

Immunocytochemistry

Cells plated in coverslips were washed two times with PBS, fixed with 4% PFA for 20 minutes at room temperature, and washed with PBS and stored at 4ºC until used. Then, cells were permeabilized for 5 minutes with 1% Triton/PBS, followed by three washes with PBS and blocked in 3% BSA/PBS for 1 hour at room temperature. Primary antibodies (Table 2) were diluted in 3% BSA/PBS and cells were incubated with them overnight at 4ºC. Then, cells were washed two times with PBS and incubated with Alexa Fluor secondary conjugated

antibodies (Table 2) at room temperature, diluted in 1% BSA/PBS. Coverslips were then washed two times with PBS, stained with DAPI (1:5000) for 5 minutes, followed by three more PBS washes. Finally, cover-slips were mounted with fluorescence mounting medium (Dako). Antibodies used are listed in Table 2.

Images were acquired at room temperature with an Axio Imager Z2 widefield microscope (CCD monochromatic digital camera Axiocam HRm) using EC Plan-Apochromat 10x/0,3NA or Plan-Apochromat 20x/0,8NA air objectives.

Table 2. Antibodies

Primary Antibodies				
Antibody	Brand	Immunocytochemisty	Immunohistochemistry	Western Blot
MAP2	Sigma-Aldrich	1:250	1:250	-
B3 tubulin (M)	Invitrogen	1:500	1:200	1:5000
B3 tubulin (R)	Cell Signaling	1:400	-	-
GFAP	DAKO	1:400	1:400	1:1000
Iba1	WAKO	-	1:500	-
Caspase 3	Cell Signaling	-	1:1000	-
S100β	Abcam	1:400	1:500	1:5000
1H9	Millipore	1:1000	-	1:1000
PSD-95	Cell Signaling	1:1000	-	1:1000
VGLUT1	Millipore	1:1000	-	-
Gephyrin	Synaptic Systems	1:500	-	-
Nanog	Cell Signaling	1:800	-	1:1000
O4	R&D systems	1:100	-	-
Oct 3/4	Santa cruz	-	-	1:1000

Sox 2	R&D systems	-	-	1:500
Actin	Sigma-Aldrich	-	-	1:1000
Nestin	R&D systems	-	-	1:1000
NG2	Millipore	1:150	-	-
Secondary Antibodies				
For Immunocytochemistry/Immunohistochemistry: Alexa Fluor (Thermo Fisher) 488, 568, 594, 647 anti-Mouse, anti-Rabbit and anti-Guinea pig; 1:250 dilution.				
For Wester Blot: Goat anti-Mouse IgG, IgM (H+L) Secondary Antibody (Thermo) and Goat anti-Rabbit IgG (H+L) Secondary Antibody (Thermo); 1:10.000 dilution.				

R: rat, M: mouse.

Total neurite length measurement and synapse quantification

Cells plated in coverslips were washed two times with PBS, fixed with 4% PFA for 20 minutes at room temperature, and washed with PBS and stored at 4ºC until used. Then, cells were permeabilized for 5 minutes in 0.25% Triton/PBS at room temperature, washed three times with PBS and blocked in 10% BSA/PBS for 1 hour. Cells were incubated overnight with the primary antibodies diluted in 3% BSA/PBS.

For excitatory synapse quantification, primary antibodies used were: rabbit anti-PSD-95 (1:1000, Cell Signalling), guinea pig anti-VGLUT1 (1:1000, Millipore) and mouse anti-MAP2 (1:250, Sigma-Aldrich). For inhibitory postsynaptic terminals quantification, primary antibodies used were: rabbit anti-β3-Tubulin (1:400, Cell Signalling) and mouse anti-Gephyrin (1:500, Synaptic Systems). The cells were washed two times with PBS followed by a 45 minutes incubation at 37ºC, with Alexa Fluor conjugated secondary antibodies diluted in 1% BSA/PBS. Coverslips were then washed two times with PBS, stained with DAPI (1:5000) for 5 minutes, followed by three more PBS washes. Coverslips were then mounted with fluorescence mounting medium (Dako).

For neurite length measurement, images were acquired at room temperature with an Axio Imager Z2 widefield microscope (CCD monochromatic digital camera Axiocam HRm) using EC Plan-Apochromat 10x/0,3NA or Plan-Apochromat 20x/0,8NA air objectives after randomly selecting MAP2-positive cellular tracts. Images were then analysed blindly to condition in Fiji software.

For synapse quantification, images were acquired at room temperature with an Axio Imager Z2 widefield microscope (CCD monochromatic digital camera Axiocam HRm) using Plan-Apochromat 63x/1,4NA after randomly selecting MAP2/ β3-Tubulin-positive cellular tracts. Images were analysed blindly to condition using Fiji software in manually thresholded images. Number of colocalized puncta, for excitatory synapses, or total number of puncta, for inhibitory postsynaptic terminals, were quantified as functional synapses normalized per dendritic section length.

Western Blot

Cells cultured as previously described were washed twice with PBS and kept at -80ºC until being processed. Cell extracts were made with lysis buffer (Table 3), vigorously vortexed and submitted to three cycles of sonication (10 seconds at 20-40 kHz). Then, samples were quantified using the BCA protein assay (Pierce) according to manufacture instructions. To samples was added loading buffer (Table 3) and denaturation was performed at 95ºC for 5 minutes. Proteins were separated by SDS-polyacrylamide gel electrophoresis (PAGE), in a 8% resolving acrylamide gel at 70V for 10 minutes and at 100V for the rest of the run. After the electrophoresis proteins were transferred to a polyvinylidene difluoride (PVDF) membrane, which has to be previously activated: 1 minute in methanol, 5 minutes in water and 5 minutes in CAPS (*N-cyclohexyl-3-aminopropanesulfonic acid*)/methanol. Transference was performed at 4ºC, 0.75 A for 2.5 hours. Membrane was blocked for 1 hour in 5% milk TBS-Tween 20 and incubated with primary antibodies diluted in 5% Milk TBS-Tween 20 overnight at 4ºC. Then, membranes were washed three times in TBS-Tween 20 (5, 10 and 15 minutes) before 2 hours incubation at room temperature with secondary antibodies, prepared in 5% Milk TBS-Tween 20. Membranes were washed three more times with PBS and incubated with the enhanced chemifluorescence substrate (ECF, Amersham Biosciences). Chemifluorescence signal was visualized in a Bio-Rad VersaDoc 3000 Imaging System. The analysis of band intensity was performed using Image J software (NIH, USA). All antibodies used in western blot are listed in Table 2.

Table 3. Western Blot buffers

Lysis Buffer: 150 mM NaCl, 50 mM Tris, 5 mM EDTA, 1% Triton, 0.5% sodium deoxycholate and 0.1% SDS fresh added with protease (Complete Mini) and phosphatase inhibitors (PhosStop Easy pack, Roche), 10 ug/ml DTT (Sigma-Aldrich) and 1mM PMSF (Sigma-Aldrich).
Loading Buffer: 0.5 M Tris-HCl pH 6,8; 10% SDS; 30% glycerol; 0.6 M DTT and bromophenol blue.

Assessment of functional neurons by single cell calcium imaging

NESCs were differentiated into neurons as previously described. Single cell calcium imaging was used to evaluate the capacity of NESCs to give rise to functional neurons. The intracellular calcium concentration is evaluated upon KCl (50 mM) depolarization and histamine (100 µM) depolarization, these being considered a marker of functional differentiated neurons and undifferentiated neural progenitors, respectively. Coverslips were washed twice in 0.1% BSA/Krebs buffer (Table 4) and incubated with 5 µM Fluo-4/AM (Invitrogen) and 0.02% pluronic acid in 0.1% BSA/Krebs buffer for 45-50 minutes at 37ºC. After incubation, the coverslips were transferred to 0.1% BSA/Krebs buffer and kept at room temperature for 10 minutes until observation. Fluo-4/AM is a calcium indicator, increasing its fluorescence excitation at 488 nm upon Ca^{2+} binding, thus increasing the fluorescence signal level. For observation, the cells were kept with 0.1% BSA/Krebs for the basal fluorescent levels measurement, performed for 4 minutes. The 50 mM KCl/Krebs (Table 4) depolarization stimulus was added for 2 minutes, followed by a 4 minute re-polarization period in 0.1% BSA/Krebs after which, the second depolarization stimulus, 100 µM histamine in 0.1% BSA/Krebs buffer, was added for 2 minutes, followed again by 4 minute re-polarization period in 0.1% BSA/Krebs buffer. Single cell calcium imaging assay was performed in a Carl Zeiss Cell Observer Spinning Disk microscope (EM-CCD Evolve Delta camera) using a Plan-Apochromat 20x/0.8NA air objectives, recording fluorescence at 488 nm for the whole experiment. Image analysis was performed in Fiji, where cell bodies were drawn and the shift in signal intensity was measured. Cells responding to potassium were identified as functional neurons while cells responding to histamine were identified as neural progenitors. Cells were considered to respond to the potassium stimulus when a 15% increase in signal (Ca^{2+} concentration) was observed, while cells that presented a histamine/potassium ratio value equal or above 1 were considered to respond to histamine, thus considered neural progenitors.

Table 4. Buffers for single cell calcium imaging

	Krebs buffer pH 7.4 (mM)	50mM KCl/Krebs pH 7.4 (mM)
NaCl	142	96
KCl	4	50
$MgCl_2$	1	1
glucose	10	10
HEPES	10	10
$NaHCO_3$	10	10
$CaCl_2$	1	1

Stereotaxic injection of NESCs

For *in vivo* experiments, immunodeficient NOD.CB17-Prkdc scid/J mice were used. The animals (postnatal days 42–46) were submitted to deep anaesthesia (ketamine/medetomidine) and received a single stereotaxic injection of 2 ul of 150 000 NESCs injected in lobule 5 of cerebellum at 0.25 ul/min. Mice were housed in sterile conditions (Ventiracks) and food and water were provided *ad libitum.* All the experiments were carried out in accordance with the European Community Council directive (86/609/ EEC) for the care and use of laboratory animals.

Tissue preparation

After induction of deep anaesthesia (ketamine/medetomidine) mice were intracardiacally perfused with 4% cold paraformaldehyde. The brains were removed and post-fixed in 4% paraformaldehyde for 24 h at 4ºC. Then were cryoprotected by incubation in 25% sucrose/PBS for 48 h at 4ºC. Then, brains were frozen at -80ºC and 25 um sagittal sections were cut using a cryostat (Thermo Fisher Scientific). Slices of entire cerebellum were collected and stored in 48-well plates as free-floating sections in PBS/0.05 mM sodium azide. The slices were stored at 4ºC until processing.

Immunohistochemistry

Animal brain sections were washed three times with PBS and blocked and permeabilized with 10% NGS (normal goat serum)/0.1% Triton in PBS for two hours. Primary antibodies were diluted in 10% NGS/0.05% triton in PBS, and sections were incubated overnight at 4ºC. After three washes in PBS, brain sections were incubated for two hours with secondary antibodies diluted in 2% NGS/PBS. Sections were then washed three times with PBS, incubated with DAPI (1:5000) for 10 minutes, and washed three more times in PBS. Brain sections were mounted in glass slides covered with gelatine, left to dry for 15 minutes at 37ºC and mounted with mowiol mounting medium. All antibodies used are listed in Table 2.

Images were acquired at room temperature with an Axio Imager Z2 widefield microscope (CCD monochromatic digital camera Axiocam HRm) using EC Plan-Apochromat 10x/0.3NA or Plan-Apochromat 20x/0.8NA air objectives. Confocal fluorescence images were obtained with and LSM 710, Axio Observer using Plan-Apochromat 20x/0.8NA objective.

DNA fragmentation (TUNEL assay)

Brain sections obtained as previously described, were stained using the in situ cell death detection kit, TMR Red (Roche), following the supplier's instructions, to investigate apoptotic cell death. A negative (no enzyme solution used) and a positive control [cerebellar sections were incubated with DNase (Qiagen) before cell death detection] were performed. Widefield fluorescence images were acquired at room temperature with an Axio Imager Z2 widefield microscope (CCD monochromatic digital camera Axiocam HRm) using EC Plan-Apochromat 10x/0.3NA or Plan-Apochromat 20x/0.8NA air objectives.

Chapter III - Results

Cell potency evaluation of Cnt and MJD patient´s iPSC-derived NESC and resulting neural cultures

To investigate whether NESCs obtained from cell reprogramming fibroblasts of control and MJD patients are good candidates to be used in cell replacement strategies, with the goal of neural repair and replacement, different parameters were evaluated in the established cell lines. NESCs were obtained from iPSCs, which were reprogrammed from fibroblasts through the lentiviral mediated expression of four reprogramming factors (C-Myc, Oct-4, Klf4 and Sox-2) (Takahashi and Yamanaka, 2006). Thus, NESCs of control (healthy) (Fig. 7A) and MJD patients (Fig. 7B) were established and maintained in culture as undifferentiated cells, capable of unlimited self-renewal and expansion.

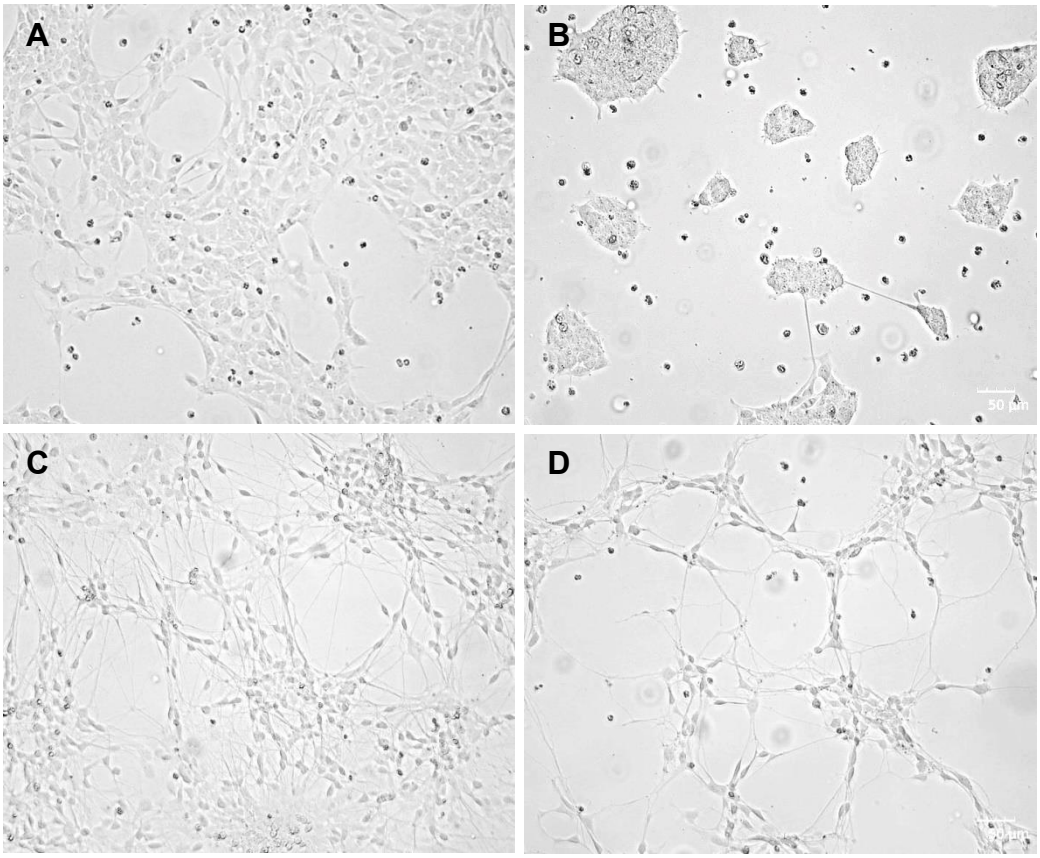

Figure 7. *Microscope evaluation* of the morphology of Control and MJD iPSCs-derived NESCs and differentiated neural cultures. Representative images of iPSCs-derived NESC cultures obtained from cell reprogramming fibroblasts of (A) Control and (B) MJD patients. Representative images of iPSCs-derived NESC from (C) Control and (D) MJD patients differentiated into neural cultures during 3 weeks.

To assess the neural multipotency of these cells, it was evaluated their ability to give rise to neural cultures upon *in vitro* differentiation. Thus, they were exposed to a differentiation protocol for three weeks, which resulted in neural cultures, with no apparent morphological

differences between cultures derived from NESCs of control (Fig. 7C) and MJD (Fig. 7D) patients. It is important to note that, in this study, a total of four cell lines (clones) were evaluated, one clone from a healthy individual (Cnt), and three clones from MJD patients (MJD-CLA, MJD-CLB and MJD-CLC).

To complement the multipotency and neuroectodermal commitment evaluation of the established lines, cell extracts of iPSCs, NESCs and neuronal cultures were analysed for pluripotency, multipotency and neuronal and glial markers (Fig. 8).

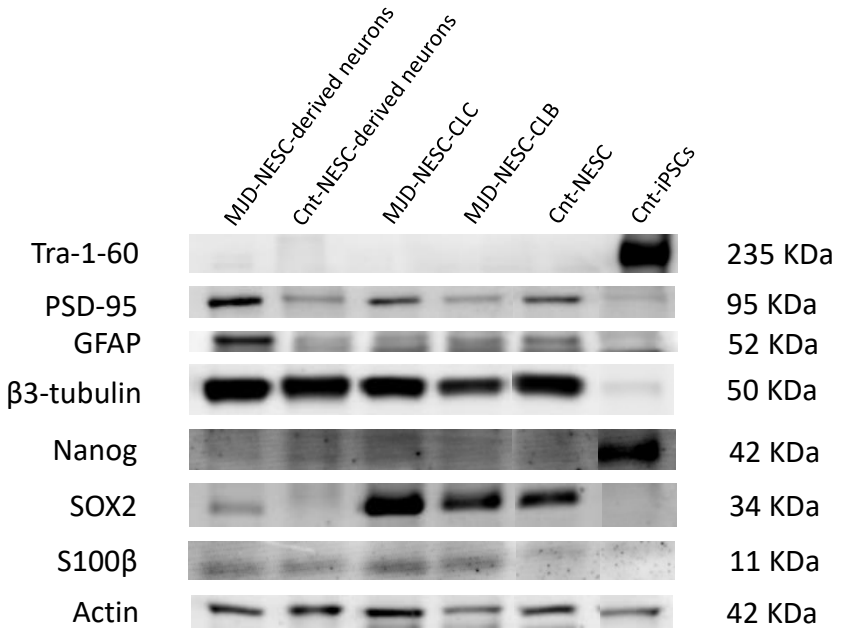

Figure 8. Evaluation of pluripotent, multipotent, neuronal and glial markers expression in iPSCs, NESCs and differentiated cultures. The protein levels of pluripotent (Nanog), neural multipotent (Sox2), neuronal (β3 tubulin and PSD-95) and glia (S100β) markers of the iPSCs, NESCs and the derived differentiated cultures were assessed by Western Blot. A) Representative image of iPSCs obtained from reprogramming fibroblasts of a Control (healthy) individual initially showed presence of pluripotent markers Nanog and Tra-1-60, which were downregulated in the derived NESCs (Cnt-NESC) and neuronal cultures (Cnt NESC-derived neurons). The MJD-patient specific iPSCs-derived NESCs (MJD-NESC) and differentiated neuronal cultures (MJD NESC-derived neurons) also have no pluripotency marker expression. Multipotent marker Sox2 was found in NESCs from both Control and MJD patients and was reduced in NESC-derived neurons. Proteins characteristic to neurons (PSD-95 and β3-tubulin) and to astrocytes (GFAP and S100B) were found in both NESCs and NESC-derived neurons.

As expected, iPSCs are positive for pluripotent markers, Nanog and Tra-1-60 that are not expressed in any other type of cells. The presence of multipotent neural stem cell marker Sox2 was also assessed, which was shown to be expressed in Cnt-NESCs and in all clones of MJD-NESCs, expression that was not present neither in iPSCs nor in Cnt-NESC-derived neural cultures. The MJD-NESC-derived neural cultures present some expression of Sox-2, although it is much small as compared to the levels expressed by NESCs. Finally, the

neuronal markers PSD-95 and β3-tubulin are expressed not only in neural cultures but also in Cnt and MJD-NESCs, whereas no expression was detected in iPSCs. Similarly to the neuronal markers, the astrocyte markers S100β and GFAP were also present in both neural cultures and NESCs, and no expression was detected in iPSCs.

The presence of mutant Ataxin-3 was expected in cells derived from MJD-patients, as they were derived from patients with the mutated *ATXN3/MJD1* gene. Thus, normal Ataxin-3 expression was detected in all Cnt and MJD-NESCs at 50 KDa (Figure 9). A band for the mutant Ataxin-3 protein, with 67KDa, was present in MJD-NESCs and MJD-NESC-derived neurons, whereas no mutant Ataxin-3 protein was found in Cnt-NESCs and Cnt-NESC-derived neural cultures (Fig. 9).

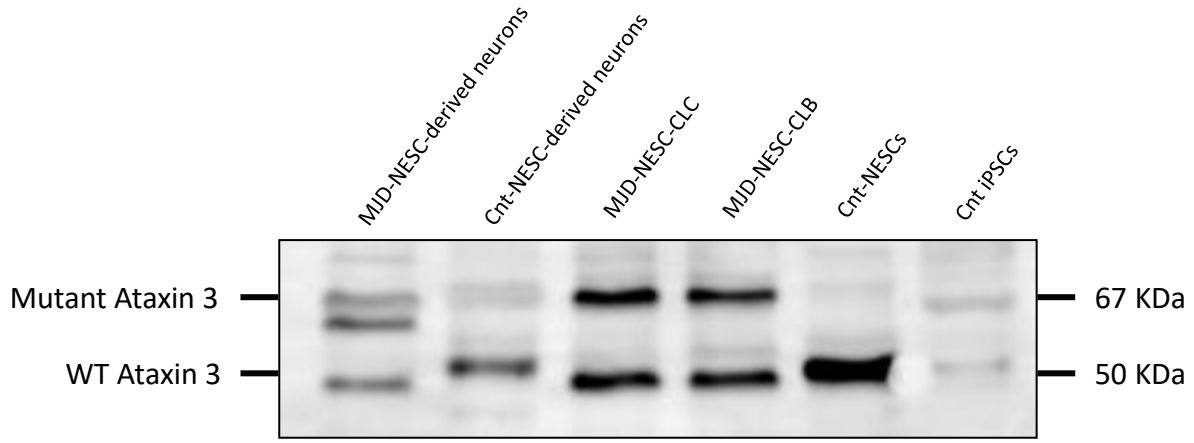

Figure 9. Evaluation of mutant Ataxin-3 in MJD-patient´s derived NESCs and differentiated cultures. Mutant Ataxin 3 is expressed in NESCs and NESC-derived neurons from MJD patients, whereas no mutant Ataxin 3 protein was found in Cnt NESCs and NESC-derived neurons.

Cnt and MJD-patient´s iPSCs-derived NESCs are capable of differentiating into neuronal and glial cells

To further evaluate the capacity of NESCs to differentiate into neuronal and glial cells, immunocytochemistry analysis was performed, after 3 weeks of exposure to differentiation medium.

Cnt-NESCs exposed to differentiation medium were capable of differentiating into a mixed culture composed by MAP2 positive neurons (Fig. 10A, B and C), as well as astrocytes, as shown by the presence of some cells labelled with the astrocyte markers S100β (Fig. 10A) and GFAP (Fig. 10B and D). Interestingly, no oligodendrocytes were present in these cultures, as no NG2 or O4 positive cells was detected (Fig 10C and D).

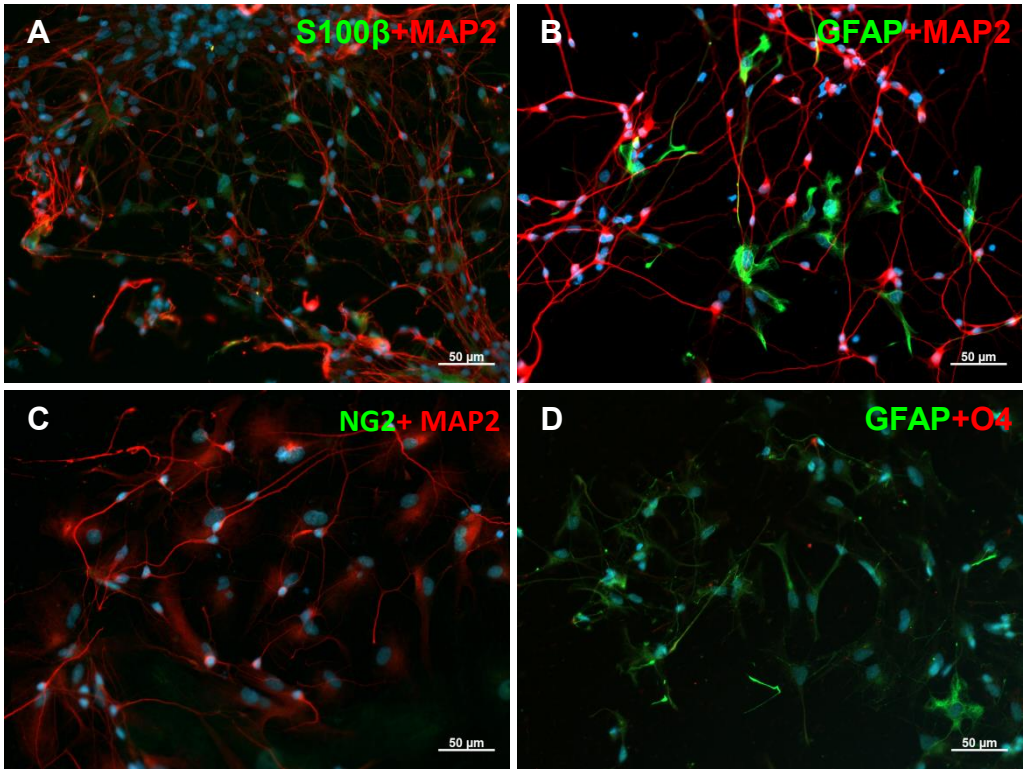

Figure 10. Control iPSC-derived NESCs differentiate into neuronal and glial cells. Immunocytochemistry of Control iPSC-derived NESCs differentiated into neural cultures for 3 weeks present (A, B and C) cells positive for neuronal (red) (MAP2) and (A, B and D) astrocytes (green) (S100B and GFAP) markers. C-D) No oligodendrocytes shown by O4 (D, Red) and NG2 (C, Green) expression was detected. Representative fluorescence images of three independent experiments.

Similar results were obtained regarding MJD-NESC-derived neuronal cultures. As for Clone A, a mixed culture of neurons and astrocytes was detected through the presence of MAP2 (Fig. 11A and B) and β3-tubulin (Fig. 11C) positive neurons and S100β (Fig. 11A) and GFAP (Fig. 11B) positive astrocytes. Once again no oligodendrocytes were detected as no NG2 (Fig. 11C) and O4 (Fig. 11D) positive cells were present. Importantly, no cells positive for the pluripotent marker Nanog (Fig. 11D) were detected.

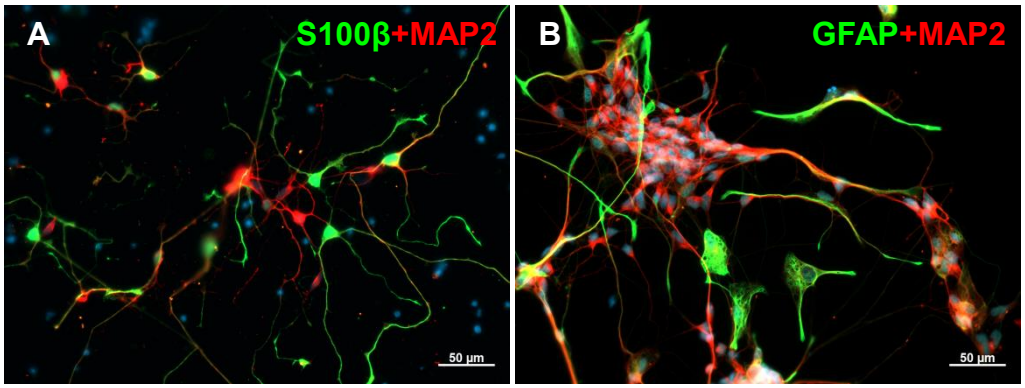

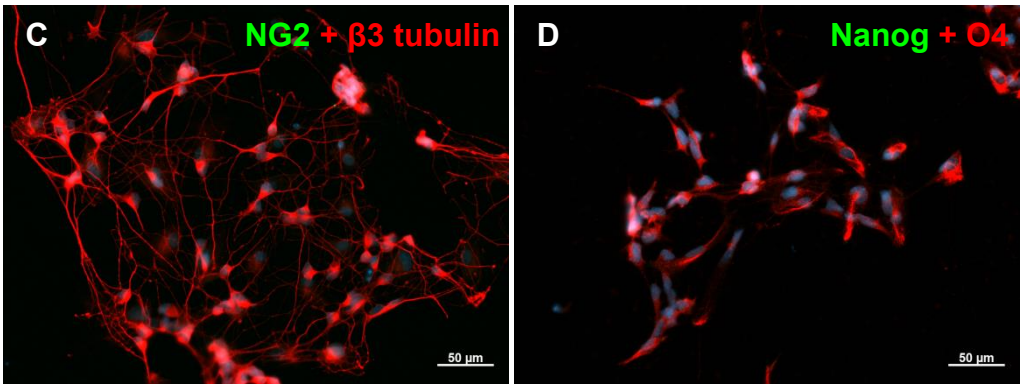

Figure 11. MJD patient´s iPSC-derived NESCs-CLA differentiate into neural and glial cells. Immunocytochemistry of MJD patient´s iPSC-derived NESCs clone A (CLA) differentiated into neural cultures for 3 weeks present (A, B and C) cells positive for neuronal (red) (MAP2 and β3-tubulin) and (A and B) astrocytes (green) (S100B and GFAP) markers. C-D) No oligodendrocytes shown by O4 (D, red) and NG2 (C, green) expression was detected. D) No expression of pluripotency marker Nanog (green) was detected. Representative fluorescence images of three independent experiments.

Regarding Clone B, mixed cultures were also obtained, containing MAP2 (Fig. 12A) and β3-tubulin (Fig. 12C and D) positive neurons, S100β (Fig. 12B) positive astrocytes and no pluripotent marker Nanog (Fig. 12D) was found. As opposed to other clones, MJD-NESCs-CLB derived cultures presented a small number of oligodendrocytes shown by the expression NG2 (Fig. 12C). Additionally, this clone also present a higher number of glia cells as compared to all the other Cnt and MJD-patient-derived established clones.

Finally, cultures obtained from MJD-NESC-CLC also differentiate into MAP2 (Fig. 13A and B) and β3-tubulin (Fig. 13D) positive neurons, GFAP (Fig. 13A and C) and S100β (Fig. 13B) positive astrocytes, and no O4 (Fig. 13C) positive oligodendrocytes were detected. Similarly, to the previous clones the pluripotent Nanog marker (Fig. 13D) was not detected.

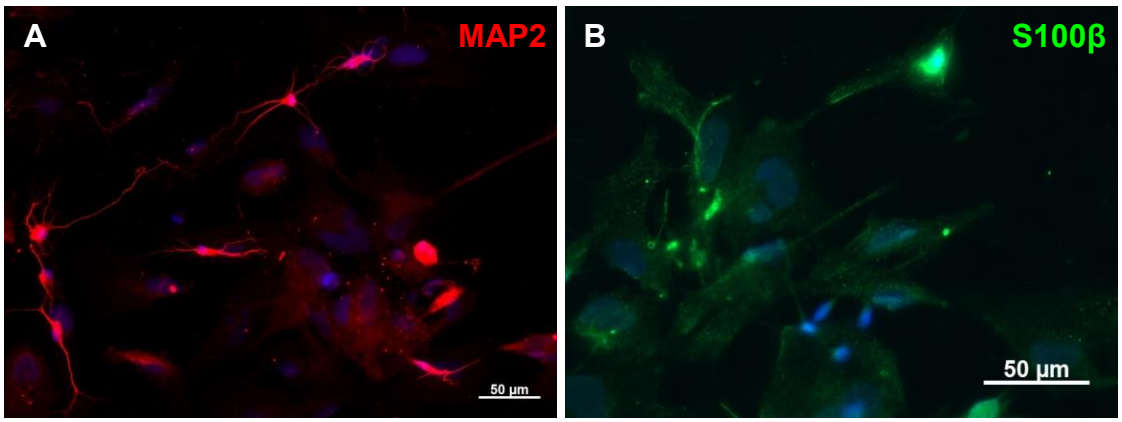

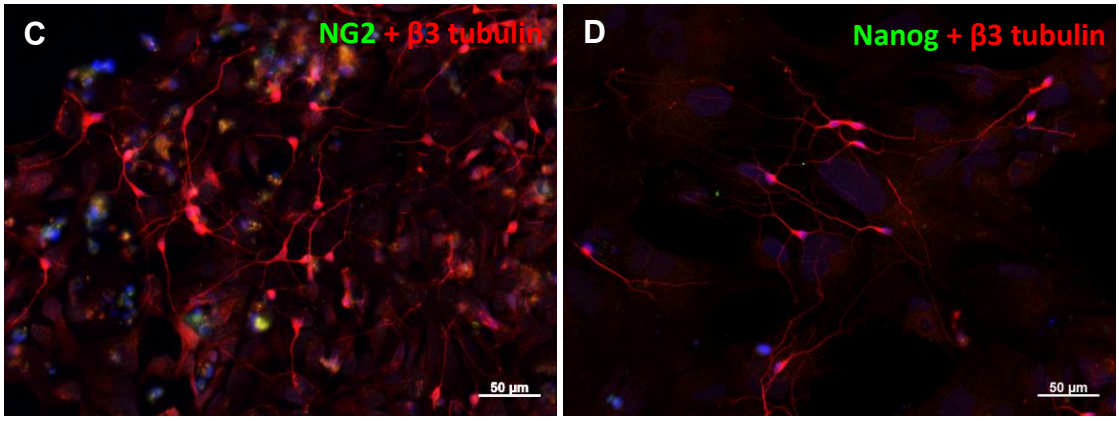

Figure 12. MJD patient´s iPSC-derived NESCs-CLB differentiate into neural and glial cells. Immunocytochemistry of MJD patient´s iPSC-derived NESCs clone B (CLB) differentiated into neural cultures for 3 weeks present (A, C and D) cells positive for neuronal (red) (MAP2 and β3-tubulin) and (B) astrocytes (green) (S100B) markers. C) A small number of oligodendrocytes revealed by expression of NG2 (green) was detected. D) No expression of pluripotency marker Nanog (green) was found. Representative fluorescence images of three independent experiments.

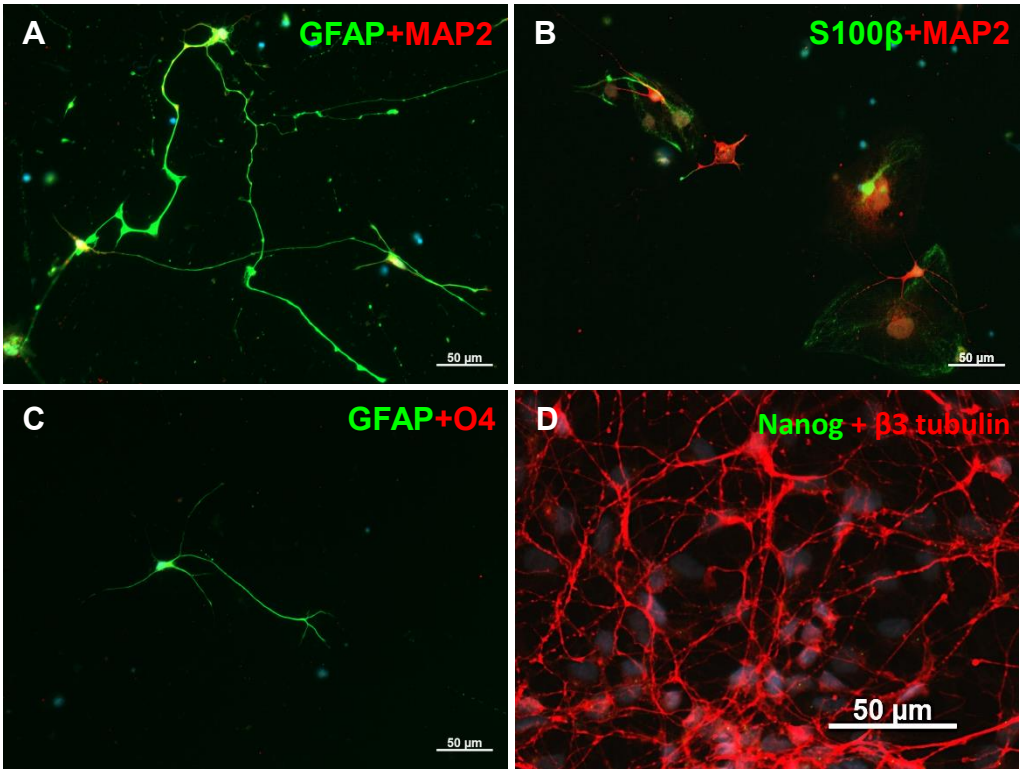

Figure 13. MJD patient´s iPSC-derived NESCs-CLC differentiate into neural and glial cells. Immunocytochemistry of MJD patient´s iPSC-derived NESCs clone C (CLC) differentiated into neural cultures for 3 weeks present (A, B and D) cells positive for neuronal (red) (MAP2 and β3-tubulin) and (A, B and C) astrocytes (green) (GFAP and S100B) markers. C) No oligodendrocytes shown by O4 (red) expression was detected. D) No expression of pluripotency marker Nanog (green) was found. Representative fluorescence images of three independent experiments.

Mutant Ataxin-3 protein has no effect on the neuronal functionality at short times

Mutant Ataxin-3 has been previously shown to affect the number of excitatory glutamatergic synapses as well as inhibitory postsynaptic terminals and to lead to dendritic loss (Koeppen et al., 1999; Konno et al., 2014; Matos et al., 2016). Thus, neurons obtained from NESCs from Cnt and MJD patients were submitted to functional evaluation tests. The number of functional excitatory glutamatergic synapses was assessed by the colocalization of puncta (Fig. 14D) of pre and post synaptic protein markers VGLUT1 (Fig. 14B) and PSD-95 (Fig. 14C) respectively, on MAP2 positive neurites (Fig. 14A). This quantification was performed in Cnt-NESC derived neurons and MJD-NESC derived neurons (CLA, CLB and CLC).

The results of this quantification are summarized in figure 14E and the values were normalized per neurite length to the mean of the Cnt. Interestingly, only MJD-NESC-CLA derived neurons showed a statistically significant reduction on the number of functional excitatory synapses when compared to the control. MJD-NESC-CLA derived neurons also proved to be significantly different to MJD-NESC-CLC derived neurons, having a smaller number of excitatory synapses. MJD-NESC-CLB and CLC derived neurons show no significant differences compared to control neurons, although there seems to be a small reduction on MJD-NESC-CLB derived neurons.

Inhibitory postsynaptic terminals were also quantified, as the total number gephyrin positive puncta (Fig. 15B) on β3-tubulin positive neurites (Fig. 15A). The number of inhibitory postsynaptic terminals, normalized per neurite length to the mean of the Cnt, demonstrated to be very similar between clones (Cnt and MJD). However, MJD-NESC-CLC derived neurons have higher numbers of inhibitory postsynaptic terminals when compared to the Cnt neurons as well as when compared to MJD-NESC-CLB (Fig. 15D).

The length of the neurites was also measured to assess whether it was affected by mutant Ataxin-3 presence. For this, on Cnt and MJD-NESC (CLA, CLB and CLC) derived neural cultures, MAP2 positive neurites (Fig. 16A) were measured and results are summarized on Figure 16B. Notably, MJD-NESC-CLC derived neurons showed to have neurites significantly longer as compared to Cnt-NESC neurons, while the other two clones (CLA and CLB) showed no difference on neurite length when compared to Cnt. Although no other differences were found when compared to control neurons, there were some differences between different clones of MJD-NESC derived neurons. MJD-NESC-CLC derived neurons presented significantly longer neurites to both MJD-NESC derived neurons of CLA and CLB.

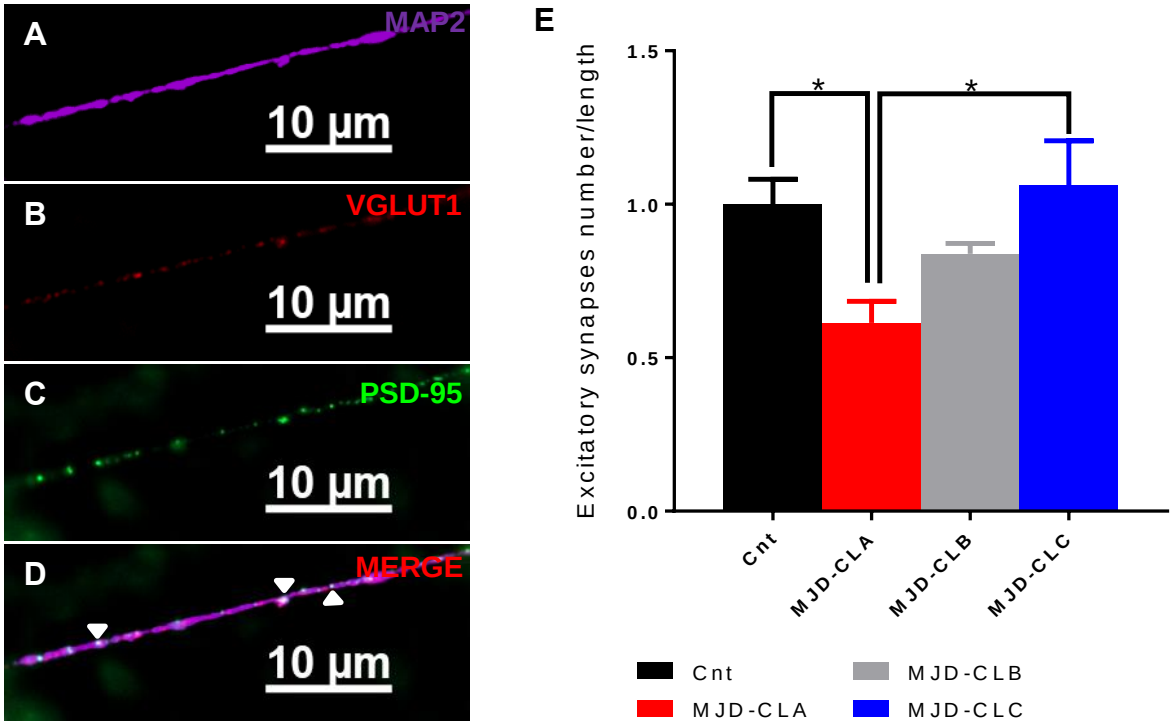

Figure 14. Quantification of excitatory synapses of neurons obtained from control and MJD patient´s iPSCs-derived NESCs. Representative immunocytochemistry image of excitatory synapses assessment on (A) MAP2 positive neurites of control and MJD patient´s iPSCs-derived NESCs differentiated into neural cultures for 3 weeks. Excitatory synapses were defined as instances of (C) PSD-95 and (B) VGLUT1 puncta colocalization (D, merge). E) Number of excitatory synapses (Cnt: n=23 neurons, from 4 independent experiments; NESC-CLA: n=21 neurons, from 3 independent experiments; NESC-CLB: n=34 neurons, from 3 independent experiments; NESC-CLC: n=17 neurons, from 2 independent experiments;) Data are expressed as mean ± SEM, *p<0.05; One way ANOVA followed by Tukey post test.

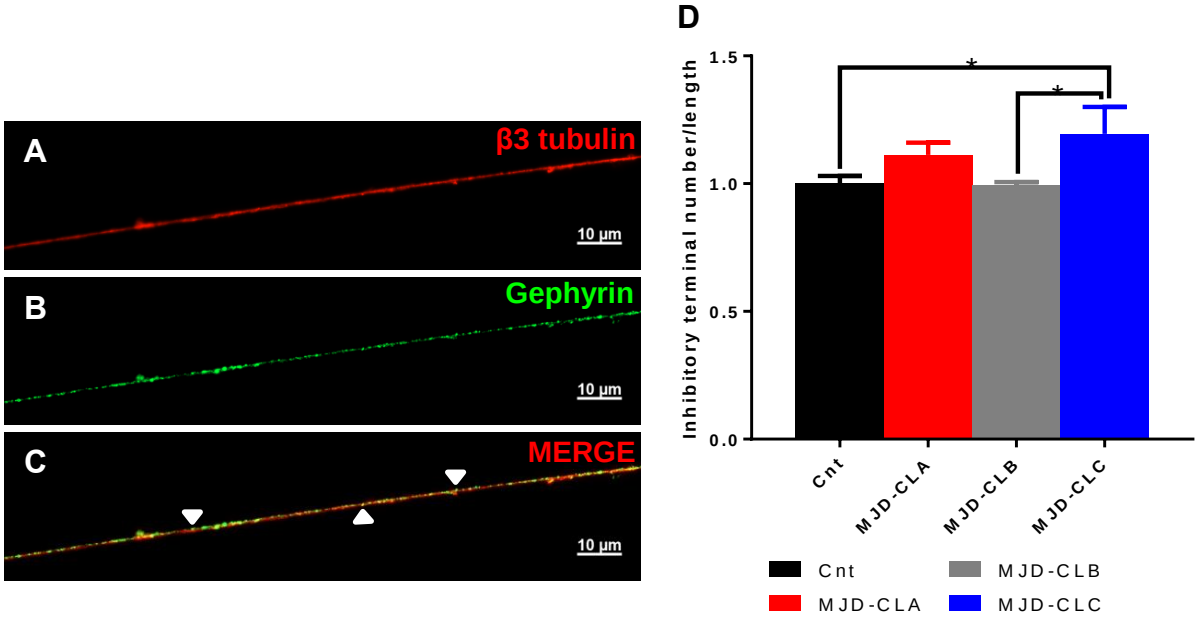

Figure 15. Quantification of inhibitory postsynaptic terminals of neurons obtained from control and MJD patient´s iPSCs-derived NESCs. Immunocytochemistry of inhibitory synapses detected and quantified on (A) β3-tubulin positive neurites of control and MJD patient´s iPSCs-derived NESCs differentiated into neural cultures for 3 weeks, as (B) Gephyrin-positive puncta. D) Number of inhibitory postsynaptic terminals (Cnt: n=40 neurons, from 4 independent experiments; NESC-CLA: n=22 neurons, from 3 independent experiments; NESC-CLB: n=41 neurons, from 3 independent experiments; NESC-CLC: n=22 neurons, from 3 independent experiments). Data are expressed as mean ± SEM, *p<0.05; One way ANOVA followed by Tukey post test.

As opposed to MJD-NESC-CLB derived neurons that presented shorter neurites than the other two clones (CLA and CLC). Looking at the number of neurites per neuron (Fig. 16C), we have some differences between the different cell lines. Neurons of MJD-NESC-CLA and CLB have significantly more neurites per neuron than the Cnt-NESC derived neurons, while neurons of MJD-NESC-CLC presented fewer neurites per neuron when compared with MJD-NESC-CLB.

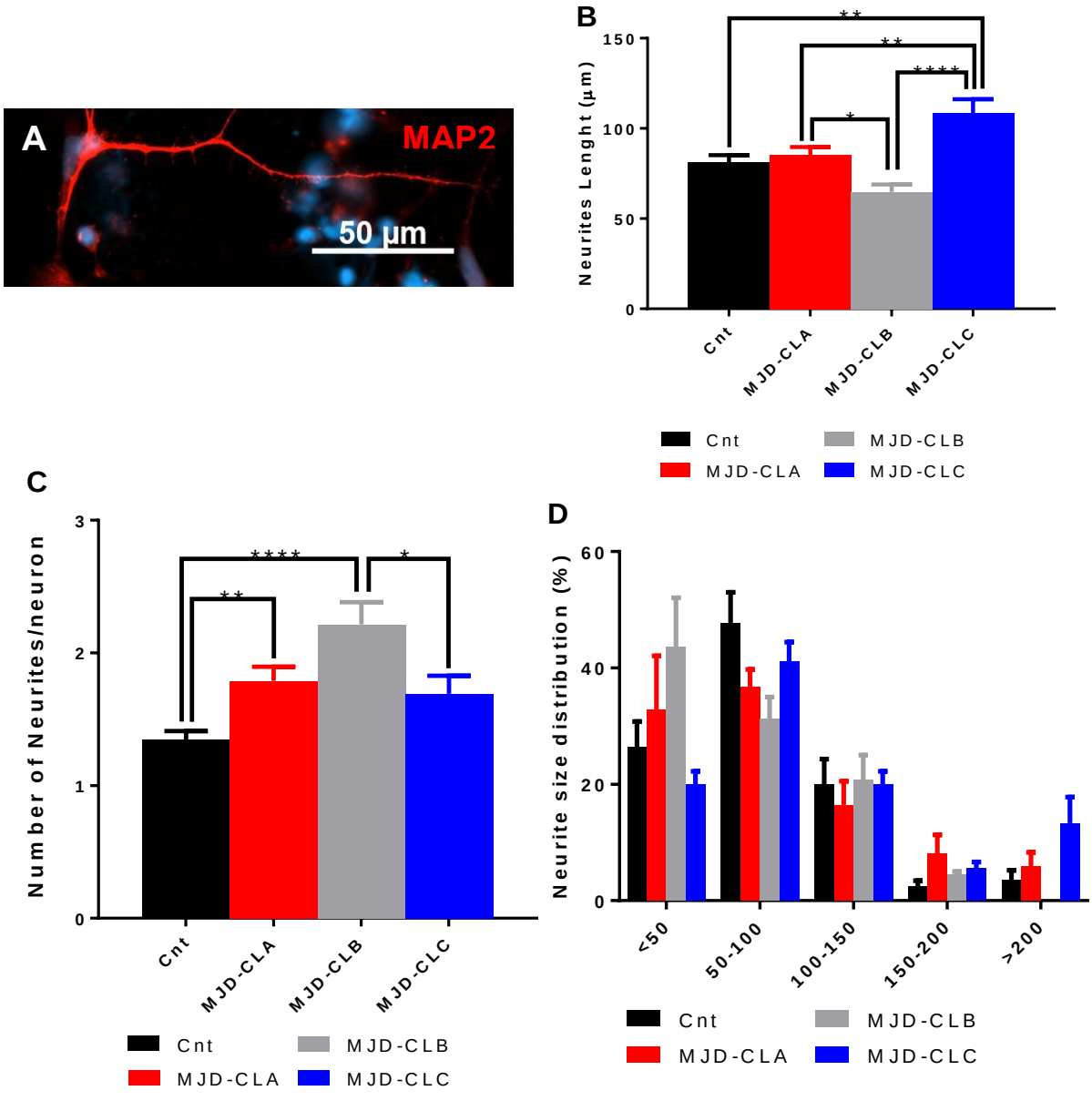

Figure 16. Total neuronal neurite length of control and MJD patient´s iPSCs-derived NESCs. A) Representative image of immunocytochemistry of MAP2 positive neurons of control and MJD patient´s iPSCs-derived NESCs differentiated into neural cultures for 3 weeks. B and C) Total neurites length and total number of neurites per neuron. D) Neurites distribution according to its length (<50, 50-100, 100-150, 150-200 and >200). (Cnt: n=95 neurons, from 5 independent experiments; NESC-CLA: n=110 neurons, from 5 independent experiments; NESC-CLB: n=43 neurons, from 2 independent experiments; NESC-CLC: n=52 neurons, from 2 independent experiments;). Data are expressed as mean ± SEM, *p<0.05, **p<0.01 and ***p<0.001; ****p<0.0001, One way ANOVA followed by Tukey post test.

To further evaluate the ability of Cnt and MJD-NESC derived neurons firing when stimulus are used we resorted to single cell calcium imaging technique. Thus, neural cultures were submitted to different stimulus and the variation of intracellular calcium was registered. A described marker of mature functional neurons is the capacity to depolarize in response to KCl stimulation. On the other hand, cells responding to a histamine stimulus correspond to undifferentiated neural progenitors (Mendonca et al., 2015). Therefore, neural cultures obtained from Cnt and MJD-NESC were submitted to these stimuli and variation of intracellular calcium was registered. Overall, when submitted to KCl stimulus, the intracellular concentration of calcium increases in neurons, as evidenced by an increase of fluorescence emitted by the calcium probe (Fig.17A and B). As opposed to KCl, the fluorescence does not significantly increases after the histamine stimulus (Fig. 17C and D).

Our results demonstrate that the obtained cultures are mostly composed by mature functional neurons, as most cells responded to the KCl stimulus (Fig. 17G). About 85% of the cells in Cnt-NESC derived neural culture responded to KCl. Similar results were observed on MJD-NESC-CLA and CLB derived neural cultures where 93% and 90% of the cells also responded to KCl stimulation, respectively. As for MJD-NESC-CLC neural cultures, the percentage of cells responding to KCl decreased to 65%, however this decrease is not statistically significant. Besides the percentage of cells responding to each stimulus, also the response intensity was evaluated (Fig. 17E and F). Likewise, no significant difference was observed between any of the neural cultures (Cnt and MJD-NESC neural cultures). Thus, iPSC-derived NESCs from both healthy (Cnt) and MJD patients were capable of giving rise to mature functional neurons upon 3 weeks of *in vitro* differentiation.

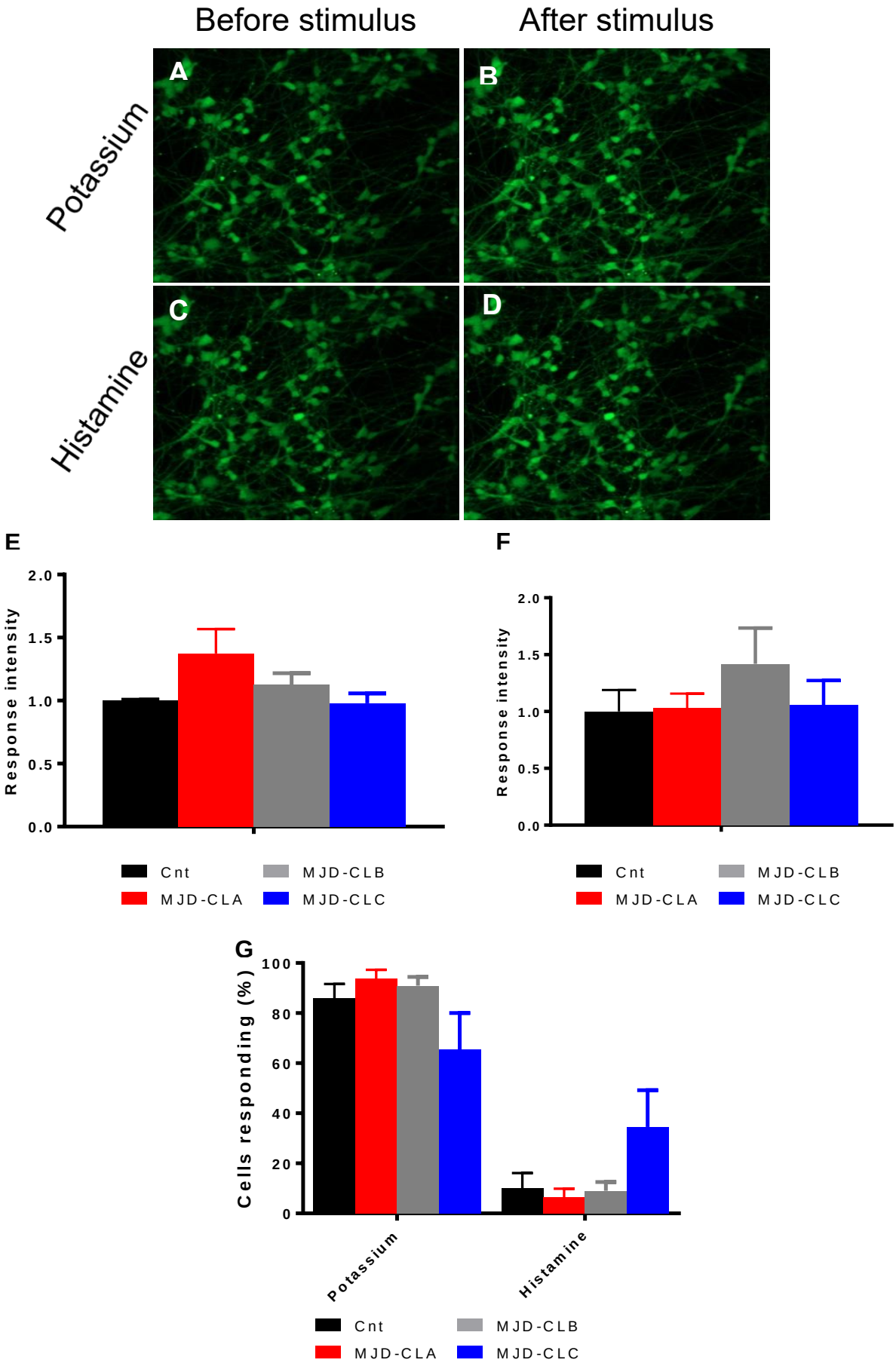
Before stimulus
After stimulus
Potassium
Histamine
A
B
C
D
E
F
G
Response intensity
2.0
1.5
1.0
0.5
0.0
Cnt
MJD-CLA
MJD-CLB
MJD-CLC
Cells responding (%)
100
80
60
40
20
0
Potassium
Histamine

Figure 17. Control and MJD patient´s iPSCs-derived NESCs differentiate into mature functional neurons. Variation of intracellular calcium concentration on neurons from control and MJD patient´s iPSCs-derived NESCs cultures, differentiated 3 weeks, evaluated through single cell calcium imaging. Representative images of fluorescence levels of the calcium indicator in cultures (A) before and after (B) KCl stimulus and (C) before and after (D) histamine stimulus. E-G) Response intensity to both KCl (E) and Histamine (F) stimulus was measured through the variation of fluorescence signal as well as percentage of cells responding to each stimulus (G). (Cnt: n=311 neurons, from 4 independent experiments; NESC-CLA: n=272 neurons, from 4 independent experiments; NESC-CLB: n=59 neurons, from 4 independent experiments; NESC-CLC: n=201 neurons, from 4 independent experiments;) Data are expressed as mean ± SEM, One way ANOVA followed by Tukey post test.

Cnt and MJD iPSC-derived NESCs survived 8 weeks after cerebellar transplantation

Following the *in vitro* characterization of Cnt and MJD iPSC derived NESC and corresponding neural cultures, Cnt and MJD-NESC-CLA were assessed for *in vivo* cell replacement potential. For this, NESCs were stereotaxically injected into the lobule 5 of the cerebellum of NOD.Scid mice after being transduced with lentiviral vectors encoding GFP to enable tracking and identification of grafted cells upon transplantation.

Eight weeks after transplantation, the survival of the transplanted cells was assessed. The transplanted Cnt-NESCs were detected (cells expressing GFP), and found to have integrated in the cerebellum and survived up to 8 weeks after transplantation (Fig. 18M) that was the longest time evaluated. To further assess the survival of the graft, apoptotic evaluation was performed. TUNEL assay demonstrated that most of the transplanted cells are not in apoptosis (Fig. 18A-I). Results that were corroborated by cleaved caspase-3 staining, an early apoptotic marker, and again no significant colocalization between cleaved caspase-3 with GFP expressing transplanted cells was detected (Fig. 18J-L).

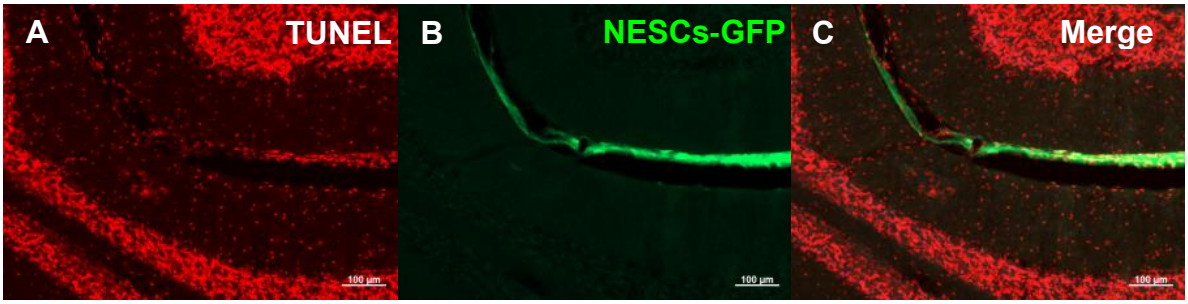

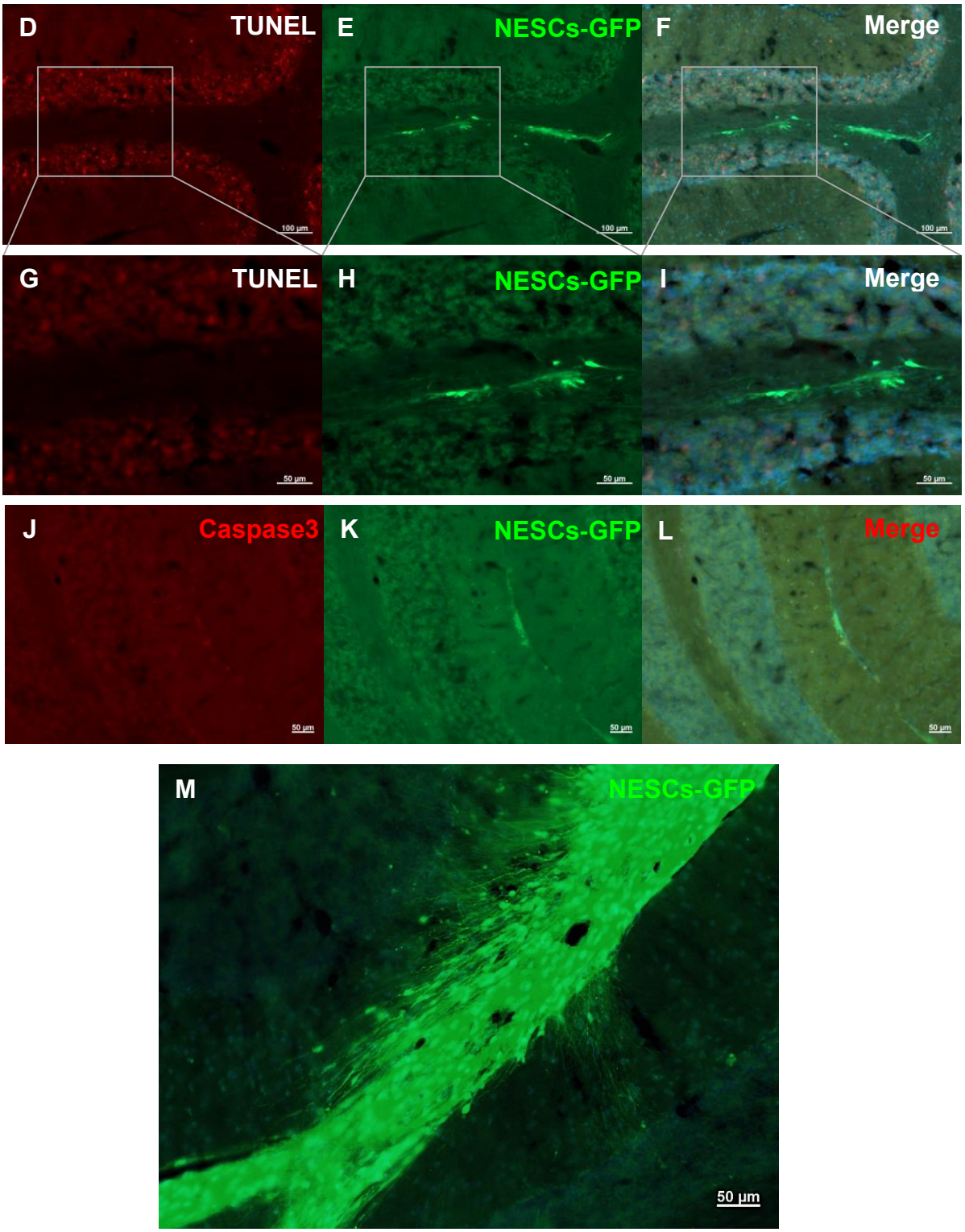

Figure 18. Control iPSCs-derived NESCs survived up to 8 weeks after cerebellar transplantation. A-M) Representative images of Control iPSCs-derived NESCs 8 weeks after transplantation into the cerebellum of adult NOD.scid mice. Apoptotic cell death evaluation with (A-I) TUNEL assay (red) and (J-L) cleaved caspase-3 reveal that the majority of the transplanted cells are not in apoptosis. A-C) Brain sections incubated with Dnase, as a positive control, resulting in an increased number of apoptotic cells (Red). D-I) Brain sections with transplanted cells stained for TUNEL assay (G, H and I are amplified images of D, E and F, respectively). J-L) Brain sections with

transplanted cells stained for cleaved caspase-3. M) Representative image of transplanted control iPSCs-derived NESCs cerebellum engraftment (n=2).

Regarding MJD-NESCs graft survival, the same tests were performed. The transplanted MJD-NESCs, also expressing GFP, were detected and found to survive and to integrate the cerebellum up to 8 weeks after transplantation (Fig. 19M), which was also the longest time evaluated. Similar to Cnt-NESCs, MJD-NESCs were submitted to TUNEL assay, which demonstrated that most of the graft does not contain apoptotic cells (Fig. 19A-I). Additionally, minor colocalization of cleaved caspase-3 with graft cells (Fig. 19J-L was observed.

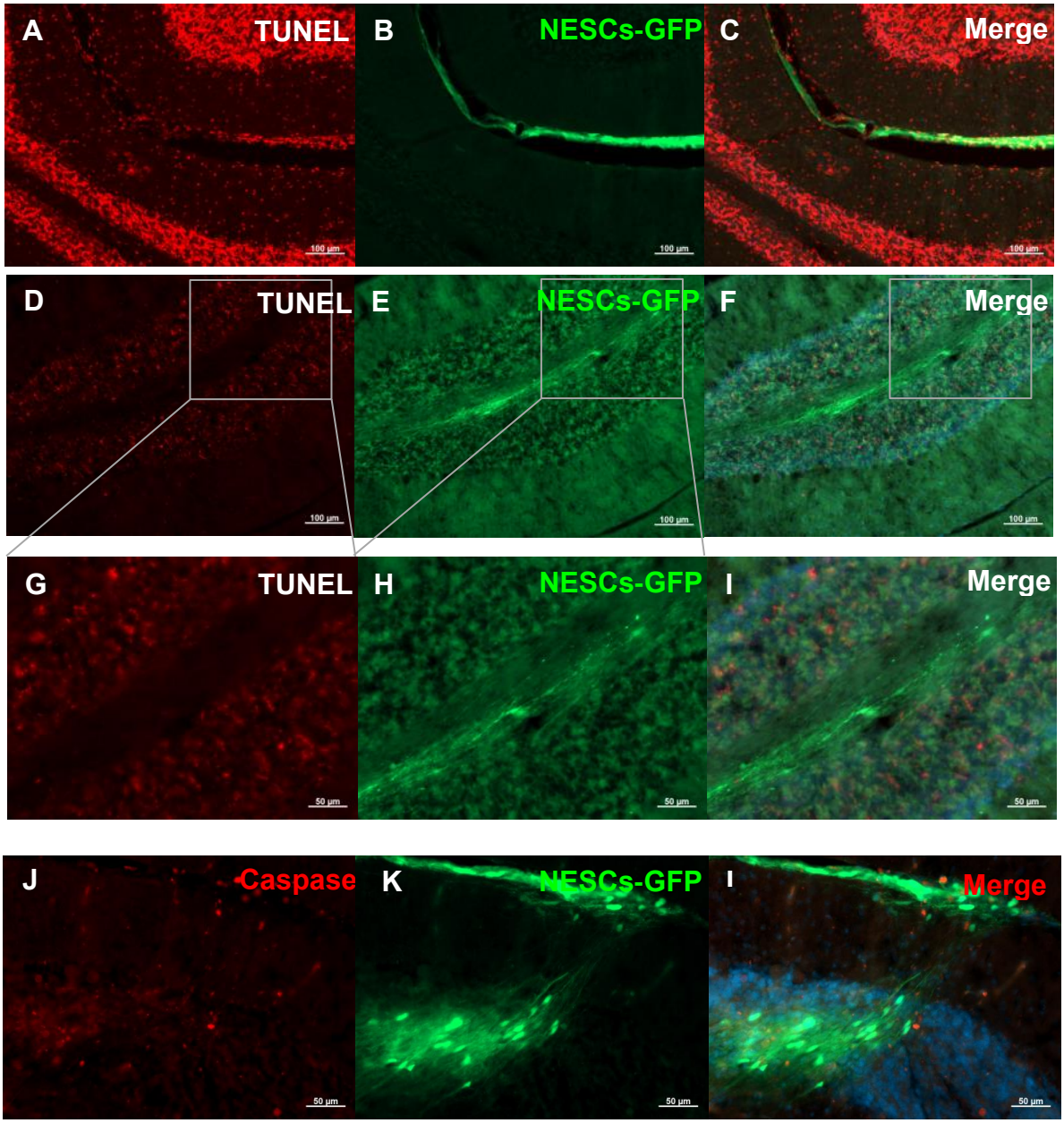

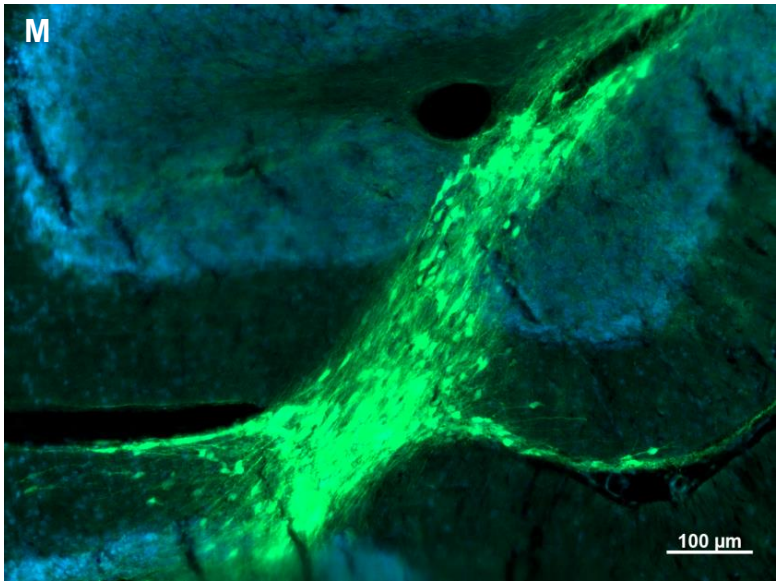

Figure 19. MJD iPSCs-derived NESCs survived up to 8 weeks after cerebellar transplantation. A-M) Representative images of MJD iPSCs-derived NESCs 8 weeks after transplantation into the cerebellum of adult NOD.scid mice. Apoptotic cell death evaluation with (A-I) TUNEL assay (red) and (J-L) cleaved caspase-3 reveal that most of the transplanted cells are not in apoptosis. A-C) Brain sections incubated with Dnase, as a positive control, resulting in an increased number of apoptotic cells (red). D-I) Brain sections with transplanted cells stained for TUNEL assay (G, H and I are amplified images of D, E and F, respectively). J-L) Brain sections with transplanted cells stained for cleaved caspase-3. M) Representative image of transplanted MJD-iPSCs-derived NECSs cerebellum engraftment (n=3).

Cnt and MJD iPSC-derived NESCs differentiate into neurons and glial cells upon cerebellar transplantation.

For an effective cell replacement strategy, transplanted cells need to be capable of differentiating into the different neural cells in the brain. Thus, cerebellar sections of NOD.Scid mice 8 weeks after transplantation were analysed to assess the capacity of Cnt and MJD-NESC differentiate into neurons and glial cells.

For this, immunohistochemical staining of cerebellar sections for neuronal and glial markers was performed. Upon transplantation, Cnt-NESCs expressing GFP were able to differentiate into MAP2 positive neurons (Fig. 20A-C) shown by the colocalization of MAP2 marker with GFP expressing cells (Fig. 20J-L). Aside from differentiating into neurons, some cells of the graft differentiated into S100β (Fig. 20G-I) and GFAP (Fig. 20D-F) positive astrocytes, verified by colocalization of GFAP marker and GFP expressing cells (Fig. 20M-P).

Additionally, NOD.Scid brain sections with transplanted MJD-NESC-CLA cells also expressing GFP were evaluated. Eight weeks post transplantation, MJD-NESCs were

capable of differentiating into MAP2 positive neurons (Fig. 21A-C) and into GFAP (Fig. 21D-F) and S100β (Fig. 21G-I) positive astrocytes.

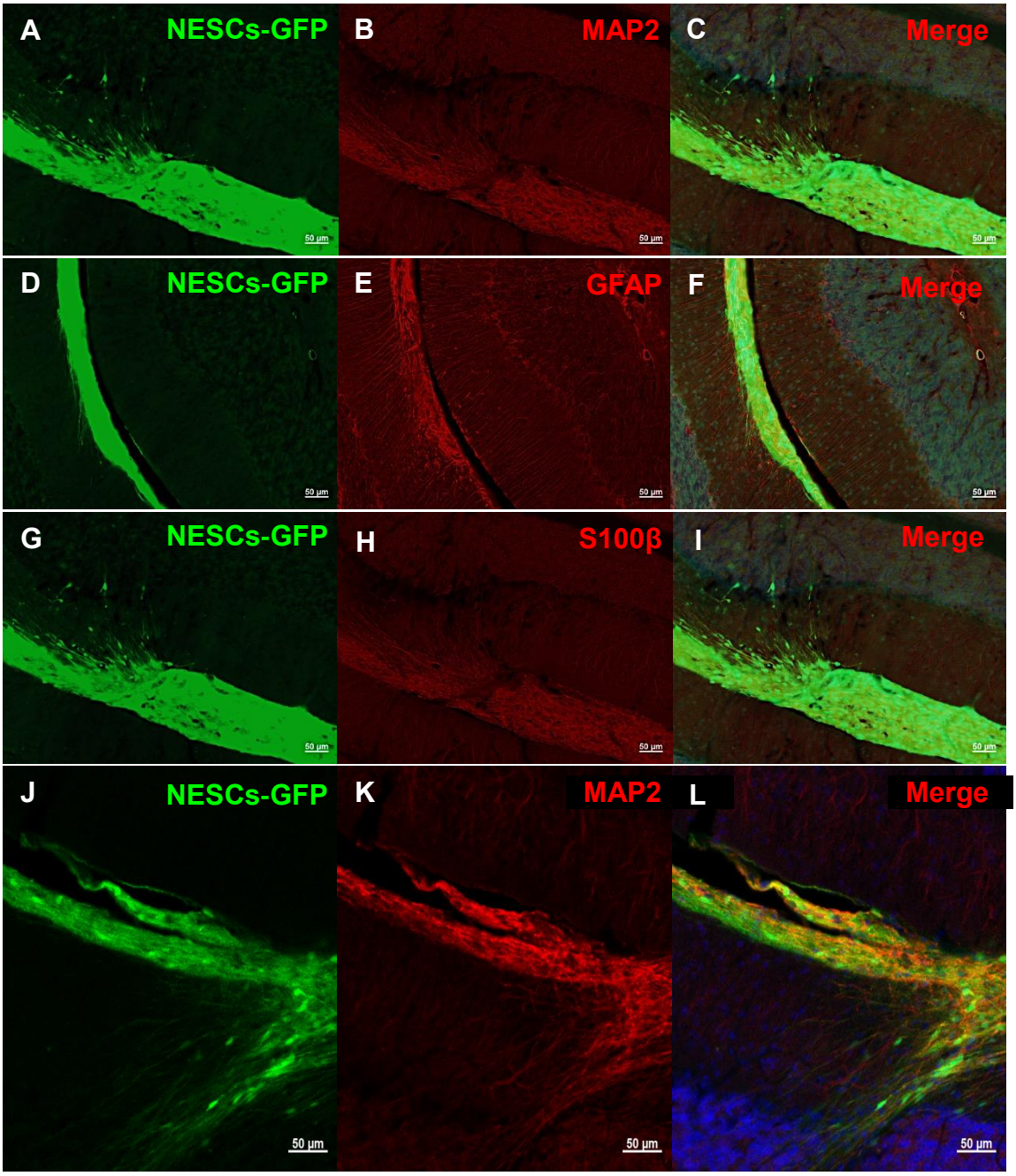

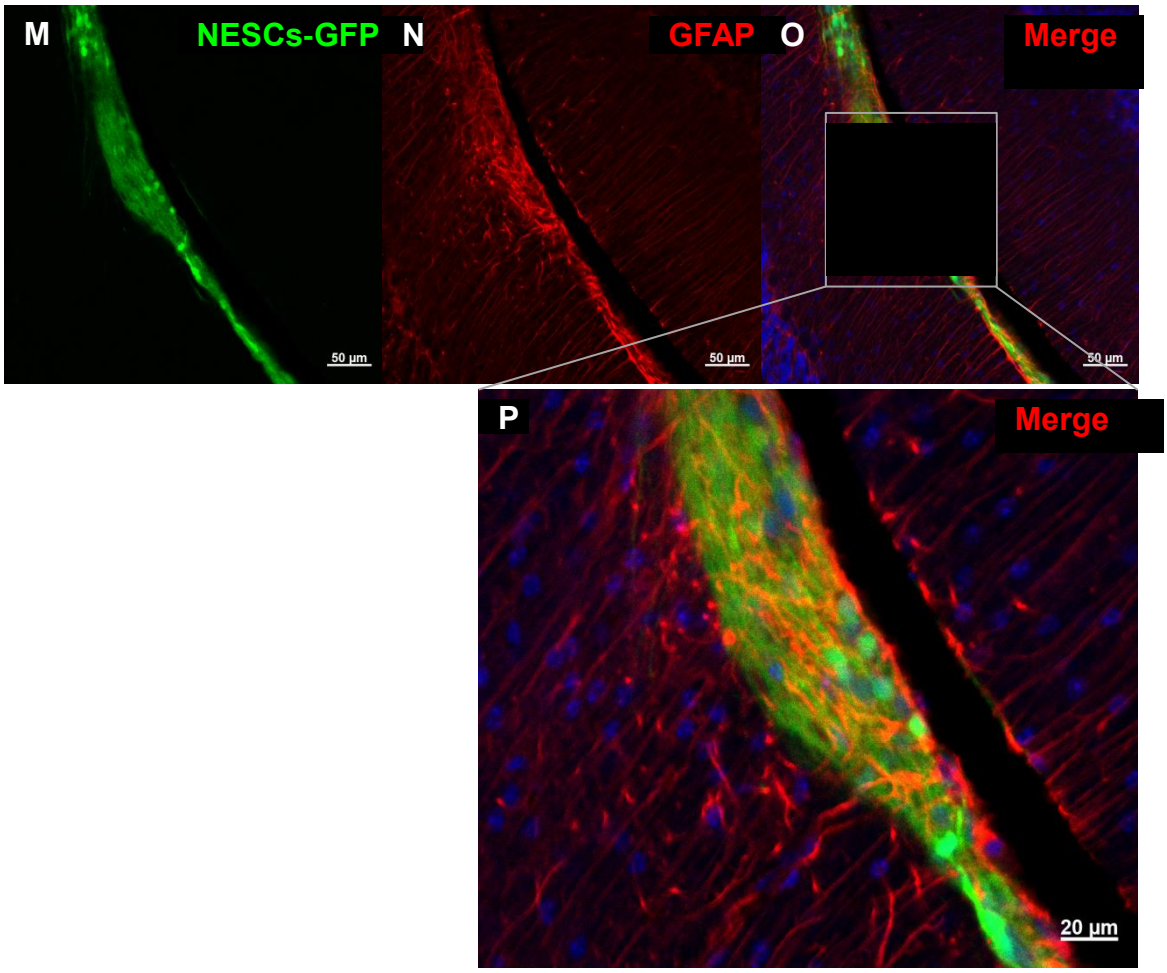

Figure 20. Control iPSCs-derived NESCs differentiate into glial cells and neurons upon transplantation. A-I) Representative images of Control iPSCs-derived NESCs 8 weeks after transplantation into the cerebellum of adult NOD.scid mice. Immunohistochemical analysis of brain sections 8 weeks after transplantation showed that the transplanted GFP-expressing cells were capable of differentiating into (A, B and C) MAP2 positive neurons and to (D, E and F) GFAP and (G, H and I) S100B positive astrocytes. J-P) Representative confocal images of control iPSCs-deeived NESCs 8 weeks after transplantation into the cerebellum of adult NOD.scid mice. Immunohistochemical analysis of brain sections 8 weeks after transplantation showed that the transplanted GFP-expressing cells were capable of differentiating into (J, K and L) MAP2 positive neurons and to (M, N, O) GFAP positive astrocytes (P is an amplified image of O) (n=3)

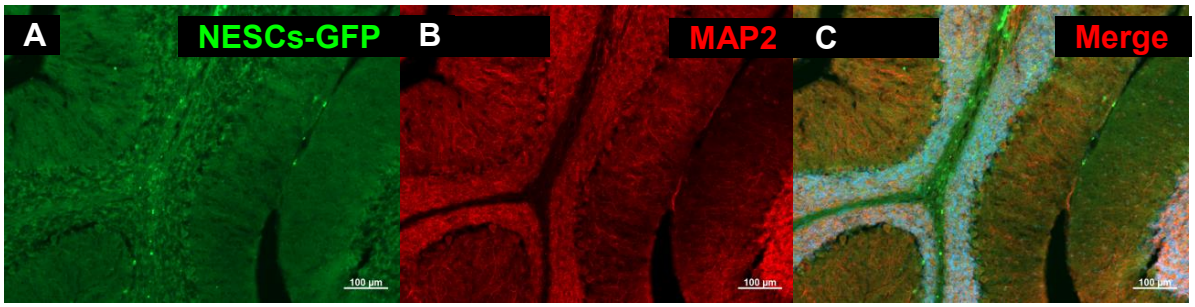

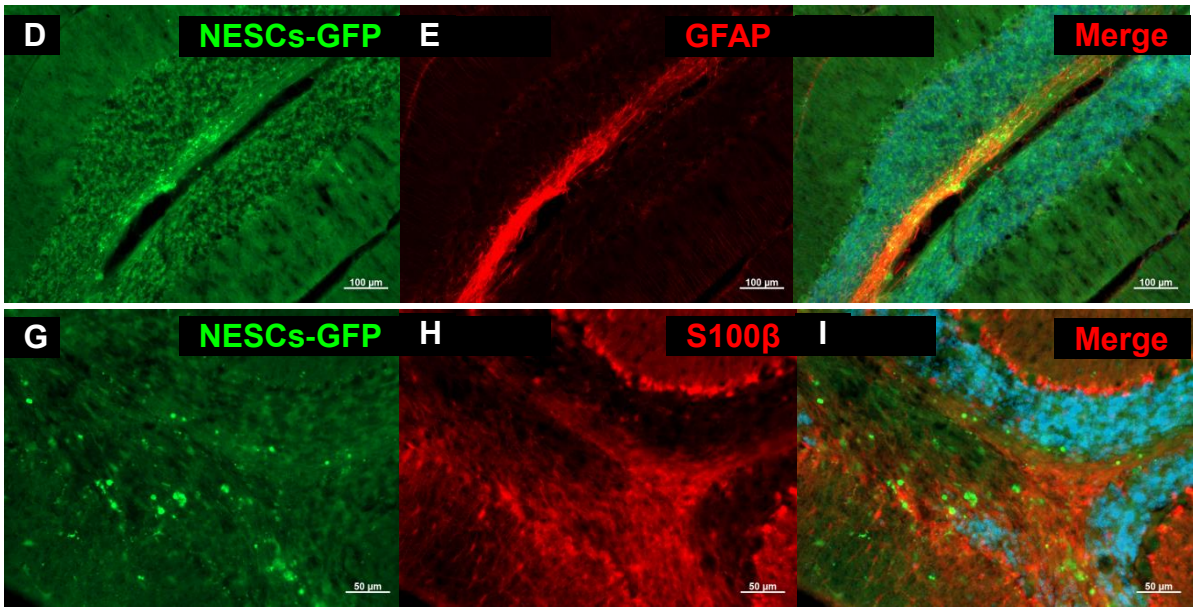

Figure 21. MJD patient´s iPSCs-derived NESCs differentiate into glial cells and neurons upon transplantation. Immunohistochemical analysis of brain sections 8 weeks after transplantation showed that the transplanted GFP-expressing cells were capable of differentiating into (A,B and C) MAP2 positive neurons and to (D, E and F) GFAP and (G, H and I) S100B positive astrocytes.

Slight neuroinflammation was triggered by NESCs transplantation

Finally, before the implementation of iPSC-derived NESC in clinical practice it is mandatory to evaluate their safety, namely their potential activation of immune rejection and major neuroinflammation.

Thus, in present work it was evaluated the neuroinflammation triggered by the transplantation of control and MJD iPSC-derived NESCs into the cerebellum of NOD.scid mice through immunohistochemical analysis. The brain sections of the transplanted mice, 8 weeks upon transplantation were assessed for microglia activation by the iba-1 marker and astrogliosis with GFAP marker. Cnt-NESCs (Fig. 22A and B) promoted very little recruiting of microglia (Fig. 22B) and GFAP positive cells (Fig. 22A) for the graft surroundings, indicating that the transplant of Cnt-NESCs resulted in minor activation of inflammatory response. Relatively to MJD-NESCs (Fig. 22C and D) it was also observed small microglia activation (Fig. 22D); however astrogliosis was clearly augmented (Fig. 22D).

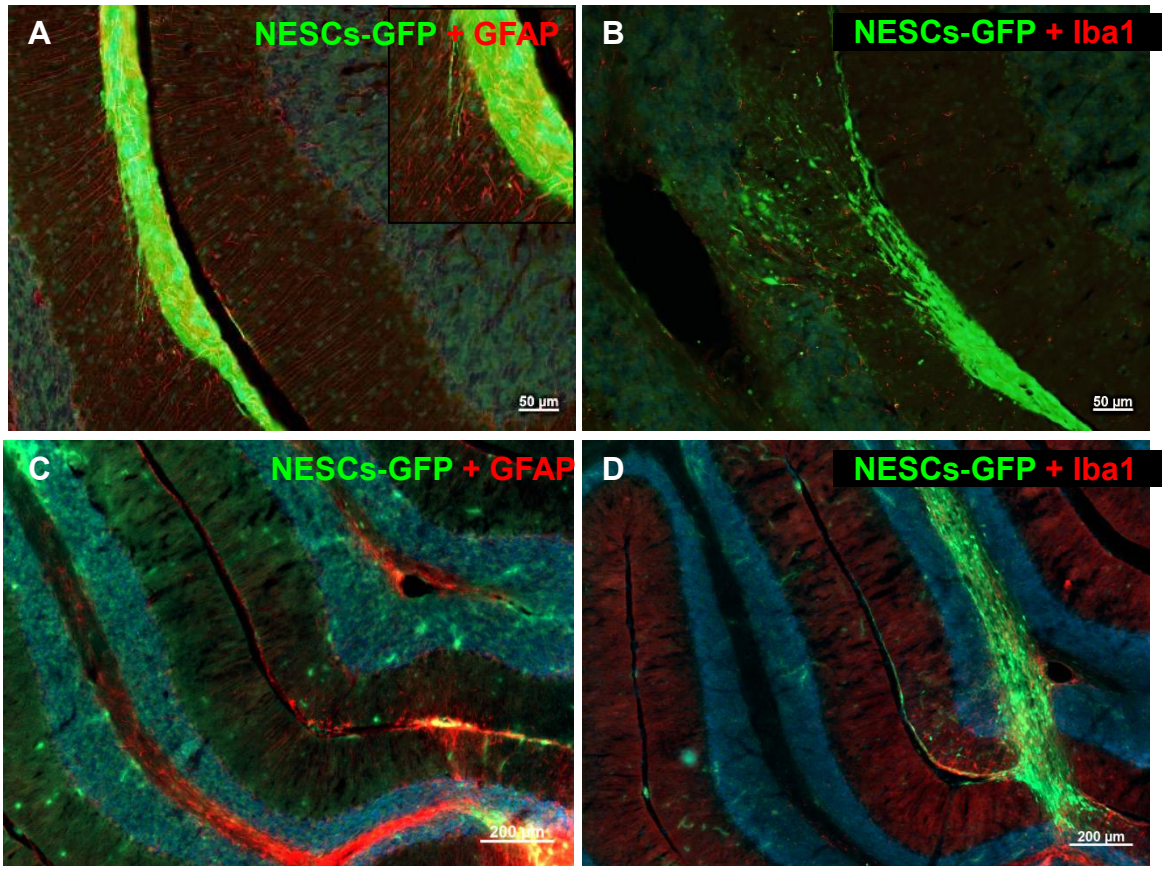

Figure 22. Neuroinflammation triggered by Control and MJD-patient´s iPSCs-derived NESCs transplantation. Representative images of neuroinflammation markers staining of (A-B) Control and (C-D) MJD patient´s iPSCs-derived NESCs 8 weeks after transplantation into the cerebellum of adult NOD.scid mice. A e C) Astrocyte marker GFAP staining and (B e D) microglia marker Iba1 staining showed a minor expression of neuroinflammation markers around the human graft.

Chapter IV - Discussion

Machado-Joseph disease is an inherited neurodegenerative disorder caused by a mutation resulting in an extended polyglutamine tract in the Ataxin-3 protein. Presently, there is no effective way to treat the disease, despite some promising approaches such as gene silencing of the mutant gene that led to alleviation of its symptoms. When patients are diagnosed an extensive neuronal loss is already present, suggesting that in combination with other approaches, cell replacement strategies might be necessary to repair neuronal damage already present at time of diagnosis. In this field, iPSCs have emerged as an ideal source of cells for cell replacement strategies, mainly by evading the ethical problems involved in the use of ESCs as well as opening the door to a more personalized medicine, avoiding possible immunological rejection by obtaining these cells from the patient that is being treated.

For this study, were used neuroepithelial stem cells established from iPSCs reprogrammed from fibroblasts of control and MJD patients. A total of four cell lines were used, one from control and three from MJD patients. Unfortunately, the second control cell line failed to be correctly established and could not be used for this study. Regarding the four established cell lines, the observed differences between them do not seem to be related to the presence of mutant Ataxin-3 in fibroblasts. In fact, the mutant protein did not affect the successful establishment of NES cell lines, in accordance with previous studies where NESCs were successfully established from fibroblasts biopsies of four MJD patients, and also no differences were apparent in NESCs obtained from both iPSCs and ESCs (Koch et al., 2011).

The cell potency characterization undertaken in this study has shown that NESCs do not have pluripotent makers, Nanog and Tra-1-60, which are present in iPSCs. This was expected since no indication of the presence of iPSCs on NESC cultures was detected, as iPSCs have a very characteristic way of growing as colonies and none were observed in growing cultures for the last year. Multipotent marker Sox2 was only detected on NESCs and appeared to have little expression on MDJ-NESC-derived neural cultures, which might be a sign that culture was not fully differentiated and still contained some multipotent cells. Neuronal and glial markers were absent in iPSCs, and were present not only in NESC-derived neural cultures but also, surprisingly, in NESCs.

The cell reprogramming method in which cells go through a pluripotent stage, as iPSCs, has been shown to reset aging markers. For example the reactivation of telomerase activity (Marion and Blasco, 2010; Rando and Chang, 2012; Wang et al., 2012) or epigenetic changes that restore chromatin state associated with aging (Meissner, 2010), pushing cells to epigenetic signatures similar to youthful cells. Since MJD is associated with aging with

increasing aggregate formation (Klockgether et al., 1999; Onodera et al., 1998), it was important to investigate whether the reprogramming of fibroblasts to iPSCs could affect the expression of mutant Ataxin-3 in reprogrammed cells from MJD patients. Here we demonstrate that NESCs and derived neural cultures continue to express mutant and wild type Ataxin-3 indicating that the reprogramming process did not affect mutant Ataxin-3 expression.

Regarding the differentiating capacity of NESCs no differences were detected between the cell lines, as Cnt and all MJD clones were capable of differentiating into neurons and astrocytes, with some oligodendrocytes being present in cultures derived from NESC-CLB. Overall, NESC-CLB have a tendency to form more glial cells than all the other clones (Cnt and MJD), this could be a result of the reprogramming process as the genetic insertion mediated by lentivirus is not controlled and it might be different in every clone, which may influence gene expression and result in differences between the clones..

Presence of mutant Ataxin-3 results in dendritic disruption of dendritic arborisation in a SCA3 mouse model (Konno et al., 2014), as well as excitatory and inhibitory synapse loss (Koeppen et al., 1999; Matos et al., 2016). Thus, we wanted to investigate whether the same differences were present in our clones, assessing neurites length and number of glutamatergic excitatory synapses and inhibitory postsynaptic terminals. Here we found some differences between clones, however the differences that were detected did not correlate to the presence of the mutation. Overall the differences that were observed were not only differences between Cnt vs MJD-NESC derived neurons but also between the three different MJD clones, suggesting that these differences are not a result of mutant Ataxin-3 presence, rather than a consequence of being different clones. However, further analysis of synaptic functionality is needed to fully assess the effects of mutant Ataxin-3.

Importantly, despite the differences observed between the clones, single cell calcium imaging showed that all clones give rise to functional mature neurons capable of responding to stimuli. Nevertheless, we speculate that some clones might need more than 3 weeks to fully mature, as is the case of MJD-NESC-CLC, which showed a lower percentage of mature neurons and a higher percentage of progenitor cells. Although this observed difference requires further investigation, given that failed to reach statistical significance.

In the *in vitro* characterization of the cell lines we could not established any correlation between the observed differences and the presence of mutant Ataxin-3. Nevertheless, possible effects mediated by its presence cannot be discarded. In fact, NESC-derived neural cultures studied were submitted to a differentiation protocol of only 3 weeks. Being MJD a

disease that has its pathological effects increased with aging (Klockgether et al., 1999; Onodera et al., 1998), besides other factors, it might be necessary to submit the cells to longer protocols for the effects of mutant Ataxin-3 to become apparent. Therefore, in this study we tried to establish a protocol to mimic the aging process by inhibiting autophagy through incubation with chloroquine. However, our preliminary studies indicate no differences in single cell calcium imaging response to stimuli with or without the authophagy inhibition. This might indicate that more than one incubation with chloroquine might be necessary to expose some effect of mutant Ataxin-3 in neuron functionality. Though this protocol is very artificial and could lead to differences that could be a result of chloroquine toxicity, which can affect the clones differently, as opposed to the presence of mutant Ataxin-3. Therefore, more tests should be performed on aged cell cultures under normal differentiating conditions, which it is possible to be performed, as we were able to maintain a NESC-derived neural culture for longer than two months.

Following *in vitro* characterization of different cell lines, we aimed to assess their potential for cell replacement strategies applied to neurodegenerative diseases. Here we demonstrated that NESCs, transplanted into the cerebellum of NOD.scid mice, were capable of surviving two months upon transplantation, the longest assessed time point in the present study. Both Cnt and MJD-NESCs were transplanted and no apparent differences were detected regarding the survival of the graft; thus more time may be needed for the negative effect of mutant Ataxin-3 protein presence to become evident. Similarly, no differences were detected regarding the differentiating capacity of the grafted cells. Both Cnt and MJD transplanted NESCs were capable of differentiating into neurons and glial cells; therefore mutant Ataxin-3 does not seem to influence NESCs differentiation upon transplantation, at least for the first two months.

After transplantation, immune rejection becomes a possible complication, which is characterized by heavy microglia activation, and astrogliosis resulting in the death of the transplanted cells (Coyne et al., 2006; Coyne et al., 2007; Finsen et al., 1991). As a result of cell death, GFP expression of transplanted cells decreases, and the absence of visible neurites engrafting the transplanted brain and the retraction of the graft are clear signs of that engraftment failed. In the present work, these signs were not present, indicating that the cells engrafted the cerebellum of the transplanted mice. However, astrogliosis was higher in brain sections of mice transplanted with MJD-NESCs. Thus, it is important to investigate if the graft is able to survive for longer periods and if this astrogliosis is a direct result of the presence of mutant Ataxin-3, as this reaction is absent around Cnt-NESC grafts and as the

presence of this mutant protein was previously shown to lead to astrogliosis (Rub et al., 2002).

Chapter V – Conclusions and future perspectives

In this work, we aimed to assess the potential of human iPSCs-derived NESCs to be used in cell replacement strategies. The use of human cells in cell replacement strategies, mainly iPSCs, has some advantages when compared to other cell types. Namely, these cells escape ethical problems associated to embryo-derived pluripotent stem cells, and hold the possibility of personalised medicine implementation, avoiding immune rejection of transplants. When patients are diagnosed with MJD, usually an extended neuronal loss is already established; thus it is necessary to replace neurons in an attempt to revert some of the damage. Here we demonstrated that all of our tested cell lines show some potential to be used as a source of cell for cell replacing strategies. Given that, all the established cell lines are multipotent and after *in vitro* differentiation and also upon brain transplantation originate neurons and glia. However, some parameters like astrogliosis presence around MJD-NESC grafts indicate that it is likely that cells obtained from MJD patients need to be submitted to mutation correction or silencing before being used for transplant. Therefore, further investigation is needed for more conclusive results. Next steps should include:

- Optimization of the aging of the NESCs-derived neural cultures, either using older cultures or optimizing the toxic stimulus protocol, in order to observe the effects of mutant Ataxin-3 in these cultures.
- Evaluation of genomic stability, through karyotyping of the tested cell lines.
- For clinical application, silencing of mutant Ataxin-3 of MJD-NESCs and respective characterization of the corrected cell lines, following transplant of these cells into the cerebellum of Nod.scid mice, and evaluation of survival and neural differentiation.
- Further evaluation of astrogliosis activation by MJD-NESCs, augmenting the number of tested animals as well as evaluation at longer time points.

Chapter VI - References

References

Alison, M.R., et al., 2000. Hepatocytes from non-hepatic adult stem cells. Nature. 406**,** 257.

Alves, S., et al., 2008a. Allele-specific RNA silencing of mutant ataxin-3 mediates neuroprotection in a rat model of Machado-Joseph disease. PLoS One. 3**,** e3341.

Alves, S., et al., 2008b. Striatal and nigral pathology in a lentiviral rat model of Machado-Joseph disease. Hum Mol Genet. 17**,** 2071-83.

Amabile, G., Meissner, A., 2009. Induced pluripotent stem cells: current progress and potential for regenerative medicine. Trends Mol Med. 15**,** 59-68.

Barre-Sinoussi, F., Montagutelli, X., 2015. Animal models are essential to biological research: issues and perspectives. Future Sci OA. 1**,** FSO63.

Bauer, P.O., Nukina, N., 2009. The pathogenic mechanisms of polyglutamine diseases and current therapeutic strategies. J Neurochem. 110**,** 1737-65.

Bernardo, M.E., Locatelli, F., Fibbe, W.E., 2009. Mesenchymal stromal cells. Ann N Y Acad Sci. 1176**,** 101-17.

Bershteyn, M., et al., 2017. Human iPSC-Derived Cerebral Organoids Model Cellular Features of Lissencephaly and Reveal Prolonged Mitosis of Outer Radial Glia. Cell Stem Cell. 20**,** 435-449 e4.

Bettencourt, C., Lima, M., 2011. Machado-Joseph Disease: from first descriptions to new perspectives. Orphanet J Rare Dis. 6**,** 35.

Biswas, D., Jiang, P., 2016. Chemically Induced Reprogramming of Somatic Cells to Pluripotent Stem Cells and Neural Cells. Int J Mol Sci. 17**,** 226.

Bjorklund, A., Lindvall, O., 2017. Replacing Dopamine Neurons in Parkinson's Disease: How did it happen? J Parkinsons Dis. 7**,** S23-S33.

Boeddrich, A., et al., 2006. An arginine/lysine-rich motif is crucial for VCP/p97-mediated modulation of ataxin-3 fibrillogenesis. EMBO J. 25**,** 1547-58.

Bohn, M.C., et al., 1987. Adrenal medulla grafts enhance recovery of striatal dopaminergic fibers. Science. 237**,** 913-6.

Budworth, H., McMurray, C.T., 2013. A brief history of triplet repeat diseases. Methods Mol Biol. 1010**,** 3-17.

Burnett, B., Li, F., Pittman, R.N., 2003. The polyglutamine neurodegenerative protein ataxin-3 binds polyubiquitylated proteins and has ubiquitin protease activity. Hum Mol Genet. 12**,** 3195-205.

Chambers, S.M., et al., 2009. Highly efficient neural conversion of human ES and iPS cells by dual inhibition of SMAD signaling. Nat Biotechnol. 27**,** 275-80.

Chen, X., et al., 2008. Deranged calcium signaling and neurodegeneration in spinocerebellar ataxia type 3. J Neurosci. 28**,** 12713-24.

Chou, A.H., et al., 2008. Polyglutamine-expanded ataxin-3 causes cerebellar dysfunction of SCA3 transgenic mice by inducing transcriptional dysregulation. Neurobiol Dis. 31**,** 89-101.

Chou, A.H., et al., 2011. HDAC inhibitor sodium butyrate reverses transcriptional downregulation and ameliorates ataxic symptoms in a transgenic mouse model of SCA3. Neurobiol Dis. 41**,** 481-8.

Citron, M., 2004. Strategies for disease modification in Alzheimer's disease. Nat Rev Neurosci. 5**,** 677-85.

Clarke, D.J., Dunnett, S.B., 1993. Synaptic relationships between cortical and dopaminergic inputs and intrinsic GABAergic systems within intrastriatal striatal grafts. J Chem Neuroanat. 6**,** 147-58.

Costa Mdo, C., Paulson, H.L., 2012. Toward understanding Machado-Joseph disease. Prog Neurobiol. 97**,** 239-57.

Coutinho, P., Andrade, C., 1978. Autosomal dominant system degeneration in Portuguese families of the Azores Islands. A new genetic disorder involving cerebellar, pyramidal, extrapyramidal and spinal cord motor functions. Neurology. 28**,** 703-9.

Cummings, C.J., et al., 1999. Mutation of the E6-AP ubiquitin ligase reduces nuclear inclusion frequency while accelerating polyglutamine-induced pathology in SCA1 mice. Neuron. 24**,** 879-92.

de Almeida, L.P., et al., 2001. Neuroprotective effect of a CNTF-expressing lentiviral vector in the quinolinic acid rat model of Huntington's disease. Neurobiol Dis. 8**,** 433-46.

Doerr, J., et al., 2017. Whole-brain 3D mapping of human neural transplant innervation. Nat Commun. 8**,** 14162.

Drouin-Ouellet, J., et al., 2017. Direct Neuronal Reprogramming for Disease Modeling Studies Using Patient-Derived Neurons: What Have We Learned? Front Neurosci. 11**,** 530.

Dunnett, S.B., et al., 1998. Striatal transplantation in a transgenic mouse model of Huntington's disease. Exp Neurol. 154**,** 31-40.

Durr, A., et al., 1996. Spinocerebellar ataxia 3 and Machado-Joseph disease: clinical, molecular, and neuropathological features. Ann Neurol. 39**,** 490-9.

Falk, A., et al., 2012. Capture of neuroepithelial-like stem cells from pluripotent stem cells provides a versatile system for in vitro production of human neurons. PLoS One. 7**,** e29597.

Fan, H.C., et al., 2014. Polyglutamine (PolyQ) diseases: genetics to treatments. Cell Transplant. 23**,** 441-58.

Fatehullah, A., Tan, S.H., Barker, N., 2016. Organoids as an in vitro model of human development and disease. Nat Cell Biol. 18**,** 246-54.

Faulkner, J., Keirstead, H.S., 2005. Human embryonic stem cell-derived oligodendrocyte progenitors for the treatment of spinal cord injury. Transpl Immunol. 15**,** 131-42.

Freeman, T.B., et al., 2000. Transplanted fetal striatum in Huntington's disease: phenotypic development and lack of pathology. Proc Natl Acad Sci U S A. 97**,** 13877-82.

Gafni, J., et al., 2004. Inhibition of calpain cleavage of huntingtin reduces toxicity: accumulation of calpain/caspase fragments in the nucleus. J Biol Chem. 279**,** 20211-20.

Giorgetti, A., et al., 2009. Generation of induced pluripotent stem cells from human cord blood using OCT4 and SOX2. Cell Stem Cell. 5**,** 353-7.

Gonzalez, F., et al., 2009. Generation of mouse-induced pluripotent stem cells by transient expression of a single nonviral polycistronic vector. Proc Natl Acad Sci U S A. 106**,** 8918-22.

Gu, W., et al., 2004. The shortest expanded allele of the MJD1 gene in a Chinese MJD kindred with autonomic dysfunction. Eur Neurol. 52**,** 107-11.

Han, F., Wang, W., Chen, C., 2014. Research progress in animal models and stem cell therapy for Alzheimer’s disease. Journal of Neurorestoratology. 2015:3**,** 11-22.

Hayashi, M., Kobayashi, K., Furuta, H., 2003. Immunohistochemical study of neuronal intranuclear and cytoplasmic inclusions in Machado-Joseph disease. Psychiatry Clin Neurosci. 57**,** 205-13.

Heiser, V., et al., 2000. Inhibition of huntingtin fibrillogenesis by specific antibodies and small molecules: implications for Huntington's disease therapy. Proc Natl Acad Sci U S A. 97**,** 6739-44.

Hou, P., et al., 2013. Pluripotent stem cells induced from mouse somatic cells by small-molecule compounds. Science. 341**,** 651-4.

Hu, W., et al., 2015. Direct Conversion of Normal and Alzheimer's Disease Human Fibroblasts into Neuronal Cells by Small Molecules. Cell Stem Cell. 17**,** 204-12.

Huangfu, D., et al., 2008. Induction of pluripotent stem cells from primary human fibroblasts with only Oct4 and Sox2. Nat Biotechnol. 26**,** 1269-75.

Huh, C.J., et al., 2016. Maintenance of age in human neurons generated by microRNA-based neuronal conversion of fibroblasts. Elife. 5.

Ichida, J.K., et al., 2009. A small-molecule inhibitor of tgf-Beta signaling replaces sox2 in reprogramming by inducing nanog. Cell Stem Cell. 5**,** 491-503.

Ichikawa, Y., et al., 2001. The genomic structure and expression of MJD, the Machado-Joseph disease gene. J Hum Genet. 46**,** 413-22.

Itskovitz-Eldor, J., et al., 2000. Differentiation of human embryonic stem cells into embryoid bodies compromising the three embryonic germ layers. Mol Med. 6**,** 88-95.

Jacobi, H., et al., 2011. The natural history of spinocerebellar ataxia type 1, 2, 3, and 6: a 2-year follow-up study. Neurology. 77**,** 1035-41.

Jana, N.R., et al., 2005. Co-chaperone CHIP associates with expanded polyglutamine protein and promotes their degradation by proteasomes. J Biol Chem. 280**,** 11635-40.

Johann, V., et al., 2007. Time of transplantation and cell preparation determine neural stem cell survival in a mouse model of Huntington's disease. Exp Brain Res. 177**,** 458-70.

Jung, D.W., Kim, W.H., Williams, D.R., 2014. Reprogram or reboot: small molecule approaches for the production of induced pluripotent stem cells and direct cell reprogramming. ACS Chem Biol. 9**,** 80-95.

Kaji, K., et al., 2009. Virus-free induction of pluripotency and subsequent excision of reprogramming factors. Nature. 458**,** 771-5.

Kim, D., et al., 2009. Generation of human induced pluripotent stem cells by direct delivery of reprogramming proteins. Cell Stem Cell. 4**,** 472-6.

Kim, J.B., et al., 2008. Pluripotent stem cells induced from adult neural stem cells by reprogramming with two factors. Nature. 454**,** 646-50.

Kim, S.U., de Vellis, J., 2009. Stem cell-based cell therapy in neurological diseases: a review. J Neurosci Res. 87**,** 2183-200.

Klement, I.A., et al., 1998. Ataxin-1 nuclear localization and aggregation: role in polyglutamine-induced disease in SCA1 transgenic mice. Cell. 95**,** 41-53.

Koch, P., et al., 2009. A rosette-type, self-renewing human ES cell-derived neural stem cell with potential for in vitro instruction and synaptic integration. Proc Natl Acad Sci U S A. 106**,** 3225-30.

Koeppen, A.H., et al., 1999. Synapses in the hereditary ataxias. J Neuropathol Exp Neurol. 58**,** 748-64.

Kokaia, Z., et al., 2012. Cross-talk between neural stem cells and immune cells: the key to better brain repair? Nat Neurosci. 15**,** 1078-87.

Konno, A., et al., 2014. Mutant ataxin-3 with an abnormally expanded polyglutamine chain disrupts dendritic development and metabotropic glutamate receptor signaling in mouse cerebellar Purkinje cells. Cerebellum. 13**,** 29-41.

Langbehn, D.R., et al., 2010. CAG-repeat length and the age of onset in Huntington disease (HD): a review and validation study of statistical approaches. Am J Med Genet B Neuropsychiatr Genet. 153B**,** 397-408.

Li, W., et al., 2016. Extensive graft-derived dopaminergic innervation is maintained 24 years after transplantation in the degenerating parkinsonian brain. Proc Natl Acad Sci U S A. 113**,** 6544-9.

Li, Y., et al., 2011. Generation of iPSCs from mouse fibroblasts with a single gene, Oct4, and small molecules. Cell Res. 21**,** 196-204.

Lindvall, O., et al., 1989. Human fetal dopamine neurons grafted into the striatum in two patients with severe Parkinson's disease. A detailed account of methodology and a 6-month follow-up. Arch Neurol. 46**,** 615-31.

Lindvall, O., Kokaia, Z., Martinez-Serrano, A., 2004. Stem cell therapy for human neurodegenerative disorders-how to make it work. Nat Med. 10 Suppl**,** S42-50.

Lo, B., Parham, L., 2009. Ethical issues in stem cell research. Endocr Rev. 30**,** 204-13.

Lombardi, M.S., et al., 2009. A majority of Huntington's disease patients may be treatable by individualized allele-specific RNA interference. Exp Neurol. 217**,** 312-9.

Maciel, P., et al., 2001. Improvement in the molecular diagnosis of Machado-Joseph disease. Arch Neurol. 58**,** 1821-7.

Manto, M.U., 2005. The wide spectrum of spinocerebellar ataxias (SCAs). Cerebellum. 4**,** 2-6.

Matos, C.A., de Macedo-Ribeiro, S., Carvalho, A.L., 2011. Polyglutamine diseases: the special case of ataxin-3 and Machado-Joseph disease. Prog Neurobiol. 95**,** 26-48.

Matos, C.A., et al., 2016. Ataxin-3 phosphorylation decreases neuronal defects in spinocerebellar ataxia type 3 models. J Cell Biol. 212**,** 465-80.

Mendonca, L.S., et al., 2015. Transplantation of cerebellar neural stem cells improves motor coordination and neuropathology in Machado-Joseph disease mice. Brain. 138**,** 320-35.

Mendonca, L.S., et al., 2018. Stem Cell-Based Therapies for Polyglutamine Diseases. Adv Exp Med Biol. 1049**,** 439-466.

Menzies, F.M., et al., 2010. Autophagy induction reduces mutant ataxin-3 levels and toxicity in a mouse model of spinocerebellar ataxia type 3. Brain. 133**,** 93-104.

Mertens, J., et al., 2015. Directly Reprogrammed Human Neurons Retain Aging-Associated Transcriptomic Signatures and Reveal Age-Related Nucleocytoplasmic Defects. Cell Stem Cell. 17**,** 705-718.

Meyer, J.R., 2008. The significance of induced pluripotent stem cells for basic research and clinical therapy. J Med Ethics. 34**,** 849-51.

Miller, V.M., et al., 2005. CHIP suppresses polyglutamine aggregation and toxicity in vitro and in vivo. J Neurosci. 25**,** 9152-61.

Moore, C.B., et al., 2010. Short hairpin RNA (shRNA): design, delivery, and assessment of gene knockdown. Methods Mol Biol. 629**,** 141-58.

Nanbo, A., Sugden, A., Sugden, B., 2007. The coupling of synthesis and partitioning of EBV's plasmid replicon is revealed in live cells. EMBO J. 26**,** 4252-62.

Nascimento-Ferreira, I., et al., 2011. Overexpression of the autophagic beclin-1 protein clears mutant ataxin-3 and alleviates Machado-Joseph disease. Brain. 134**,** 1400-15.

Nascimento-Ferreira, I., et al., 2013. Beclin 1 mitigates motor and neuropathological deficits in genetic mouse models of Machado-Joseph disease. Brain. 136**,** 2173-88.

Nobrega, C., et al., 2015. Re-establishing ataxin-2 downregulates translation of mutant ataxin-3 and alleviates Machado-Joseph disease. Brain. 138**,** 3537-54.

Nóbrega, C., Almeida, L.P.d., 2012. Machado-Joseph Disease / Spinocerebellar Ataxia Type 3. In: Spinocerebellar Ataxia. Vol., J. Gazulla, ed.^eds. InTech, pp. 103-115.

Okita, K., et al., 2008. Generation of mouse induced pluripotent stem cells without viral vectors. Science. 322**,** 949-53.

Olanow, C.W., et al., 2003. A double-blind controlled trial of bilateral fetal nigral transplantation in Parkinson's disease. Ann Neurol. 54**,** 403-14.

Paulson, H.L., Fischbeck, K.H., 1996. Trinucleotide repeats in neurogenetic disorders. Annu Rev Neurosci. 19**,** 79-107.

Paulson, H.L., et al., 1997. Machado-Joseph disease gene product is a cytoplasmic protein widely expressed in brain. Ann Neurol. 41**,** 453-62.

Paulson, H.L., 2007. Dominantly inherited ataxias: lessons learned from Machado-Joseph disease/spinocerebellar ataxia type 3. Semin Neurol. 27**,** 133-42.

Paulson, H.L., 2009. The spinocerebellar ataxias. J Neuroophthalmol. 29**,** 227-37.

Piccini, P., et al., 1999. Dopamine release from nigral transplants visualized in vivo in a Parkinson's patient. Nat Neurosci. 2**,** 1137-40.

Pluchino, S., et al., 2005. Neurosphere-derived multipotent precursors promote neuroprotection by an immunomodulatory mechanism. Nature. 436**,** 266-71.

Pluchino, S., et al., 2009. Human neural stem cells ameliorate autoimmune encephalomyelitis in non-human primates. Ann Neurol. 66**,** 343-54.

Poppe, D., et al., 2018. Genome Editing in Neuroepithelial Stem Cells to Generate Human Neurons with High Adenosine-Releasing Capacity. Stem Cells Transl Med. 7**,** 477-486.

Primo, M.N., Bak, R.O., Mikkelsen, J.G., 2012. Lentiviral vectors for cutaneous RNA managing. Exp Dermatol. 21**,** 162-70.

Ranum, L.P., et al., 1994. Molecular and clinical correlations in spinocerebellar ataxia type I: evidence for familial effects on the age at onset. Am J Hum Genet. 55**,** 244-52.

Reinhardt, P., et al., 2013. Derivation and expansion using only small molecules of human neural progenitors for neurodegenerative disease modeling. PLoS One. 8**,** e59252.

Rippon, H.J., Bishop, A.E., 2004. Embryonic stem cells. Cell Prolif. 37**,** 23-34.

Rub, U., Brunt, E.R., Deller, T., 2008. New insights into the pathoanatomy of spinocerebellar ataxia type 3 (Machado-Joseph disease). Curr Opin Neurol. 21**,** 111-6.

Rubinsztein, D.C., et al., 1996. Phenotypic characterization of individuals with 30-40 CAG repeats in the Huntington disease (HD) gene reveals HD cases with 36 repeats and apparently normal elderly individuals with 36-39 repeats. Am J Hum Genet. 59**,** 16-22.

Schols, L., et al., 2004. Autosomal dominant cerebellar ataxias: clinical features, genetics, and pathogenesis. Lancet Neurol. 3**,** 291-304.

Schulz, J.B., et al., 2010. Visualization, quantification and correlation of brain atrophy with clinical symptoms in spinocerebellar ataxia types 1, 3 and 6. Neuroimage. 49**,** 158-68.

Seidel, K., et al., 2010. Axonal inclusions in spinocerebellar ataxia type 3. Acta Neuropathol. 120**,** 449-60.

Shao, L., Wu, W.S., 2010. Gene-delivery systems for iPS cell generation. Expert Opin Biol Ther. 10**,** 231-42.

Shi, Y., et al., 2008a. Induction of pluripotent stem cells from mouse embryonic fibroblasts by Oct4 and Klf4 with small-molecule compounds. Cell Stem Cell. 3**,** 568-74.

Shi, Y., et al., 2008b. A combined chemical and genetic approach for the generation of induced pluripotent stem cells. Cell Stem Cell. 2**,** 525-8.

Simoes, A.T., et al., 2012. Calpastatin-mediated inhibition of calpains in the mouse brain prevents mutant ataxin 3 proteolysis, nuclear localization and aggregation, relieving Machado-Joseph disease. Brain. 135**,** 2428-39.

Simoes, A.T., et al., 2014. Calpain inhibition reduces ataxin-3 cleavage alleviating neuropathology and motor impairments in mouse models of Machado-Joseph disease. Hum Mol Genet. 23**,** 4932-44.

Somoza, R., et al., 2010. Intranigral transplantation of epigenetically induced BDNF-secreting human mesenchymal stem cells: implications for cell-based therapies in Parkinson's disease. Biol Blood Marrow Transplant. 16**,** 1530-40.

Steinbeck, J.A., et al., 2012. Human embryonic stem cell-derived neurons establish region-specific, long-range projections in the adult brain. Cell Mol Life Sci. 69**,** 461-70.

Steinbeck, J.A., Studer, L., 2015. Moving stem cells to the clinic: potential and limitations for brain repair. Neuron. 86**,** 187-206.

Takahashi, K., Yamanaka, S., 2006. Induction of pluripotent stem cells from mouse embryonic and adult fibroblast cultures by defined factors. Cell. 126**,** 663-76.

Takiyama, Y., et al., 1993. The gene for Machado-Joseph disease maps to human chromosome 14q. Nat Genet. 4**,** 300-4.

Tropepe, V., et al., 2001. Direct neural fate specification from embryonic stem cells: a primitive mammalian neural stem cell stage acquired through a default mechanism. Neuron. 30**,** 65-78.

Tzvetkov, N., Breuer, P., 2007. Josephin domain-containing proteins from a variety of species are active de-ubiquitination enzymes. Biol Chem. 388**,** 973-8.

Uchida, N., et al., 2012. Human neural stem cells induce functional myelination in mice with severe dysmyelination. Sci Transl Med. 4**,** 155ra136.

van Alfen, N., et al., 2001. Intermediate CAG repeat lengths (53,54) for MJD/SCA3 are associated with an abnormal phenotype. Ann Neurol. 49**,** 805-7.

Vierbuchen, T., et al., 2010. Direct conversion of fibroblasts to functional neurons by defined factors. Nature. 463**,** 1035-41.

Vitale, A.M., Wolvetang, E., Mackay-Sim, A., 2011. Induced pluripotent stem cells: a new technology to study human diseases. Int J Biochem Cell Biol. 43**,** 843-6.

Wang, W., et al., 2008. Chromosomal transposition of PiggyBac in mouse embryonic stem cells. Proc Natl Acad Sci U S A. 105**,** 9290-5.

Wang, Z., et al., 2013. Protective effects of BDNF overexpression bone marrow stromal cell transplantation in rat models of traumatic brain injury. J Mol Neurosci. 49**,** 409-16.

Warren, L., et al., 2010. Highly efficient reprogramming to pluripotency and directed differentiation of human cells with synthetic modified mRNA. Cell Stem Cell. 7**,** 618-30.

Wernig, M., et al., 2008. Neurons derived from reprogrammed fibroblasts functionally integrate into the fetal brain and improve symptoms of rats with Parkinson's disease. Proc Natl Acad Sci U S A. 105**,** 5856-61.

Wolfgang, W.J., et al., 2005. Suppression of Huntington's disease pathology in Drosophila by human single-chain Fv antibodies. Proc Natl Acad Sci U S A. 102**,** 11563-8.

Woltjen, K., et al., 2009. piggyBac transposition reprograms fibroblasts to induced pluripotent stem cells. Nature. 458**,** 766-70.

Xia, H., et al., 2004. RNAi suppresses polyglutamine-induced neurodegeneration in a model of spinocerebellar ataxia. Nat Med. 10**,** 816-20.

Xie, Y., Hayden, M.R., Xu, B., 2010. BDNF overexpression in the forebrain rescues Huntington's disease phenotypes in YAC128 mice. J Neurosci. 30**,** 14708-18.

Xu, L., et al., 2011. Dual transplantation of human neural stem cells into cervical and lumbar cord ameliorates motor neuron disease in SOD1 transgenic rats. Neurosci Lett. 494**,** 222-6.

Xu, Q., et al., 2013. Intrathecal transplantation of neural stem cells appears to alleviate neuropathic pain in rats through release of GDNF. Ann Clin Lab Sci. 43**,** 154-62.

Yamada, M., et al., 2001. Involvement of the cerebral cortex and autonomic ganglia in Machado-Joseph disease. Acta Neuropathol. 101**,** 140-4.

Yamada, M., et al., 2008. CAG repeat disorder models and human neuropathology: similarities and differences. Acta Neuropathol. 115**,** 71-86.

Yu, J., et al., 2009. Human induced pluripotent stem cells free of vector and transgene sequences. Science. 324**,** 797-801.

Yuan, X., et al., 2011. Brief report: combined chemical treatment enables Oct4-induced reprogramming from mouse embryonic fibroblasts. Stem Cells. 29**,** 549-53.

Zhang, L., et al., 2015. Small Molecules Efficiently Reprogram Human Astroglial Cells into Functional Neurons. Cell Stem Cell. 17**,** 735-747.

Zhou, H., et al., 2009. Generation of induced pluripotent stem cells using recombinant proteins. Cell Stem Cell. 4**,** 381-4.

Zhou, W., Freed, C.R., 2009. Adenoviral gene delivery can reprogram human fibroblasts to induced pluripotent stem cells. Stem Cells. 27**,** 2667-74.

Zhu, S., et al., 2010. Reprogramming of human primary somatic cells by OCT4 and chemical compounds. Cell Stem Cell. 7**,** 651-5.

Zhuchenko, O., et al., 1997. Autosomal dominant cerebellar ataxia (SCA6) associated with small polyglutamine expansions in the alpha 1A-voltage-dependent calcium channel. Nat Genet. 15**,** 62-9.